

Nonreciprocal tripartite entanglement and asymmetric Einstein-Podolsky-Rosen steering via directional quantum squeezing

Ya-Feng Jiao,^{1,2} Jie Wang,³ Dong-Yang Wang,⁴ Lei Tang,⁵ Yan Wang,^{1,2}
Yun-Lan Zuo,⁶ Wan-Su Bao,^{7,*} Le-Man Kuang,^{2,3,†} and Hui Jing^{2,3,‡}

¹*School of Electronics and Information, Zhengzhou University of Light Industry, Zhengzhou 450001, China*

²*Academy for Quantum Science and Technology, Zhengzhou University of Light Industry, Zhengzhou 450001, China*

³*Key Laboratory of Low-Dimensional Quantum Structures and Quantum Control of Ministry of Education, Department of Physics and Synergetic Innovation Center for Quantum Effects and Applications, Hunan Normal University, Changsha 410081, China*

⁴*School of Physics, Zhengzhou University, Zhengzhou 450001, China*

⁵*College of Physics and Electronic Engineering, Institute of Solid State Physics, Sichuan Normal University, Chengdu 610101, China*

⁶*School of Physics and Chemistry, Hunan First Normal University, Changsha 410205, China*

⁷*Henan Key Laboratory of Quantum Information and Cryptography, IEU, Zhengzhou 450001, China*

(Dated: September 11, 2024)

The generation and manipulation of multipartite entanglement and EPR steering in macroscopic systems not only play a fundamental role in exploring the nature of quantum mechanics, but are also at the core of current developments of various nascent quantum technologies. Here we report a theoretical method using directional injection of quantum squeezing to produce nonreciprocal multipartite entanglement and EPR steering in a three-mode optomechanical system with closed-loop coupling. We show that by directionally applying a two-photon parametric driving field with a phase-matched squeezed vacuum reservoir to an optomechanical resonator, a squeezed optical mode can be introduced for one of its input directions, thereby yielding an asymmetric enhancement of optomechanical interaction and the time-reversal symmetry breaking of the system. Based on this feature, it is found that bipartite and tripartite entanglement and the associated EPR steering of the subsystems can only be generated when the coherent driving field input from the squeezing injection direction, namely, achieving nonreciprocity in such quantum correlations. More excitingly, it is also found that by properly adjusting the squeezing parameter, the overall asymmetry of EPR steering can be stepwise driven from no-way regime, one-way regime to two-way regime. These findings, holding promise for preparing rich types of entangled quantum resources with nonreciprocal correlations, may have potential applications in the area of quantum information processing such as quantum secure direct communication and one-way quantum computing.

I. INTRODUCTION

Entanglement, allowing perfectly correlated positions and momenta for two spatially separated particles, has long been intriguing in quantum physics and enables numerous advanced quantum information protocols spanning from quantum networking to quantum sensing [1]. The concept of entanglement was originally addressed by Schrödinger [2] in his response to the issue of the “spooky action-at-a-distance” predicted by Einstein, Podolsky, and Rosen (EPR) in their famous paradox [3], where he also coined a term that came to be known as the EPR steering [4, 5]. From the perspective of violations of local-hidden-state models, Wiseman *et al.* has formalized an operational benchmark for EPR steering [6], by which they further proved that under the hierarchy of quantum nonlocality, EPR steering is a strict subset of entanglement and a strict superset of Bell nonlocality. An appealing feature of EPR steering is that it describes how local measurements on one part of the system can steer (alter) the state of the other part at a different location. This defining characteristics, not held by the other two types of quantum nonlocality, reveals the intrinsic asymmetry of EPR steering and

offers an insight into directional nonlocality [7], which plays an indispensable role in enabling quantum techniques using untrusted devices [8], such as secure quantum key distribution [9, 10], randomness certification [11], and no-cloning quantum teleportation [12, 13]. In the past few decades, after a series of rigorous mathematical characterizations of quantum nonlocality [14–17], a great deal of progresses have been made experimentally to prepare entangled or steerable states of microscopic and macroscopic particles, involving platforms based on photons [18], ions [19], atoms [20], superconducting circuits [21], and cavity optomechanical (COM) devices [22–24]. However, in terms of generation and manipulation of macroscopic entanglement, it is still challenging to avoid the decoherence effect induced by device imperfection. Very recently, to overcome this obstacle and achieve entangled state with high fidelity, a large number of theoretical proposals have been raised, which relies on synthetic gauge field [25, 26], reservoir engineering [27–29], dark-mode or feedback control [30–32], photon counting [33], dynamical modulation [34, 35], and optical nonreciprocity [36–38].

In parallel, nonreciprocal optical devices, such as optical diodes and circulators, have attracted intense interests due to their potential applications in the next-generation photonic information processing [39]. The conventional approach for achieving nonreciprocal transmission of light mainly relies on magneto-optical effect [40], which requires magnetic-based materials that are bulk and quite lossy at optical frequency. In

* bws@qiclab.cn

† lmkuang@hunnu.edu.cn

‡ jinghui73@gmail.com

recent years, by breaking the time-reversal symmetry [41] via spatial-temporal modulation, optical nonlinearity or Sagnac effect, several magnetic-free schemes have been theoretically proposed and experimentally demonstrated based on atomic ensembles [42–44], optical [45–47] or COM [48–50] devices, synthetic structures [51, 52], moving medium [53–55], and squeezing injection [56]. With these advances, the peculiar feature of nonreciprocal optical devices, allowing the flow of light from one side but block it from the other, has recently been employed to realize the unidirectional manipulation of light-matter interaction, which enables a variety of classical nonreciprocal phenomena, such as one-way optical chaos [57] or solitons [58], unidirectional phonon [59] or magnon [60] lasing, and nonreciprocal enhancement optomechanical sidebands [61], to name a few. Very recently, this functionality has also been extended into the quantum regime to achieve nonreciprocal control of diverse nonclassical effects, such as photon [62–64] or magnon [65] blockade, microscopic [66–68] or macroscopic [36–38] entanglement, quantum phase transition [69, 70], and EPR steering [71–73].

Inspired by these studies, we investigate how to achieve nonreciprocal entanglement and asymmetric EPR steering in a hybrid COM system based on whispering-gallery-mode (WGM) resonator. We show that by applying a two-photon parametric driving field from one input direction while not applying it from the other, the two degenerate counterpropagating optical modes of the WGM resonator can be unidirectionally squeezed, leading to the time-reversal symmetry breaking of the system. Based on this chiral squeezing characteristics, we show that various types of bipartite entanglement of the subsystems and the tripartite entanglement of the whole system can be generated only when coherent light input from the squeezing injection direction, which indicates the achievement of nonreciprocal entanglement. More interestingly, by properly adjusting the squeezing parameters, we further show that the directionality of EPR steering can also be stepwise driven from no-way regime, one-way regime to two-way regime in an asymmetric way. These results, opening up a promising way to prepare entangled quantum resources with nonreciprocal and asymmetric features, are useful for a variety of secure quantum information protocols [9–13].

This paper is structured as follows. In Sec. II, we introduce the theoretical model of the proposed COM system and obtain the effective Hamiltonian and master equation of this system, by which we calculate the system dynamics and evaluate the quantitative measures for entanglement and EPR steering. In Sec. III, based on the numerical simulations, we analyze the method and mechanism for achieving nonreciprocal generation and manipulation of various types of entanglement and EPR steering. In Sec. IV, a brief summary is given. The detailed derivation process of the effective Hamiltonian, the associated master equation, and the system dynamics is given in the Appendix.

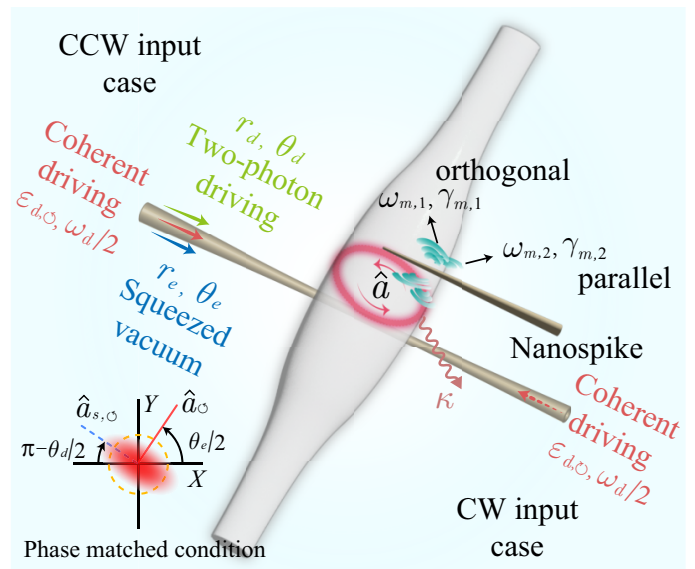


FIG. 1. Schematic of the proposed COM setup consisting of a bottle WGM resonator, an optical waveguide, and a tapered glass-fiber nanopike. The WGM resonator supports two degenerate counter-propagating optical modes, i.e., CW and CCW modes. The optical driving field is input from the waveguide, which can be coupled into and out of the WGM resonator via evanescent coupling. When placing a nanopike close to the WGM resonator, it excites two mechanical modes due to the COM interaction induced by the WGM evanescent field, whose vibrating directions are parallel and orthogonal to the resonator surface, respectively. To achieve nonreciprocal manipulation of quantum entanglement and EPR steering, we consider two different scenarios for the CW and CCW input cases. For the CW input case, only a coherent driving field is applied, while for the CCW input case, an additional two-photon parametric driving field with a phase-matched squeezed vacuum reservoir is applied.

II. THEORETICAL MODEL AND SYSTEM DYNAMICS

The proposed setup consists of a bottle WGM resonator, an optical waveguide, and a tapered glass-fiber nanopike, which is depicted in Fig. 1. Due to the spatial symmetry of the bottle WGM resonator, it can support two degenerate counter-propagating optical modes with resonance frequency ω_c , i.e., the clockwise (CW) and counterclockwise (CCW) modes, respectively. The nanopike is usually fabricated by scanning an oxybutane flame along the length of a glass fiber while gently pulling it. As demonstrated in the recent experiments [74–76], by mounting such nanopike on a stainless-steel holder and placing it close to the bottle WGM resonator, it offers two mechanical modes due to the WGM evanescent field induced COM interaction. These two mechanical modes with frequency $\omega_{m,j}$ ($j = 1, 2$) are vibrating in the directions that are orthogonal and parallel to the bottle surface, and they are coupled linearly due to the optically mediated hybridization effect [77, 78]. The WGM resonator can be driven from both sides, where the optical driving fields from the waveguide are coupled into and out of the WGM resonator via evanescent coupling.

In addition, we consider two different scenarios for the driv-

ing fields applied from the CW and CCW input directions, respectively. For the CCW input case, a coherent driving field with frequency $\omega_d/2$ and a two-photon parametric driving field with frequency ω_d are simultaneously applied to the waveguide. In this situation, in a rotating reference frame with respect to the driving frequency $\omega_d/2$, the Hamiltonian of the whole system can be expressed as (setting $\hbar = 1$)

$$\begin{aligned}\hat{H}_\circ &= \hat{H}_{\text{sys}} + \hat{H}_{\text{dr},\circ}, \\ \hat{H}_{\text{sys}} &= \Delta_c \hat{a}_\circ^\dagger \hat{a}_\circ + \sum_{j=1,2} \left[\frac{\omega_{m,j}}{2} (\hat{p}_j^2 + \hat{q}_j^2) - g_j \hat{a}_\circ^\dagger \hat{a}_\circ \hat{q}_j \right] \\ &\quad + \chi \hat{q}_1 \hat{q}_2, \\ \hat{H}_{\text{dr},\circ} &= \Xi_d (e^{-i\theta_d} \hat{a}_\circ^{\dagger 2} + e^{i\theta_d} \hat{a}_\circ^2) + i\varepsilon_{d,\circ} (\hat{a}_\circ^\dagger - \hat{a}_\circ),\end{aligned}\quad (1)$$

where \hat{a}_\circ (\hat{a}_\circ^\dagger) is the annihilation (creation) operator of the CCW mode, while \hat{q}_j and \hat{p}_j are the dimensionless displacement and momentum operators of the j th mechanical mode, respectively. $\Delta_c = \omega_c - \omega_d/2$ denotes the optical detuning, and ω_c is the resonance frequency of the CCW (CW) mode. $g_j = (\omega_c/R) \sqrt{\hbar/m_j \omega_{m,j}}$ is the single-photon COM coupling strength, with R the bottle radius and m_j the effective mass of the j th mechanical mode. χ is the mechanical coupling strength. Ξ_d and θ_d are the amplitude and phase of the two-photon parametric driving field. The amplitude of the coherent driving field is given by $|\varepsilon_{d,\circ}| = \sqrt{2\kappa P_d/\hbar\omega_d}$, where P_d is the input laser power and κ is the optical decay rate.

After performing the Bogoliubov transformation with a unitary operator, $S(\eta_d) = \exp[(-\eta_d \hat{a}_\circ^{\dagger 2} + \eta_d^* \hat{a}_\circ^2)/2]$, a squeezed optical mode $\hat{a}_{s,\circ}$ can be introduced, i.e.,

$$S^\dagger(\eta_d) \hat{a}_\circ S(\eta_d) = \cosh(r_d) \hat{a}_{s,\circ} - e^{-i\theta_d} \sinh(r_d) \hat{a}_{s,\circ}^\dagger, \quad (2)$$

where $\eta_d = r_d e^{-i\theta_d}$ is the complex squeezing parameter, with a squeezing strength r_d and a squeezing reference angle θ_d . Hence, by dropping the constant terms, the effective Hamiltonian of the total system in the squeezing picture is derived as [see Appendix A for more details]

$$\begin{aligned}\hat{H}_\circ &= \omega_s \hat{a}_{s,\circ}^\dagger \hat{a}_{s,\circ} + \sum_{j=1,2} \left[\frac{\omega_{m,j}}{2} (\hat{p}_j^2 + \hat{q}_j^2) - \zeta_{s,j} \hat{a}_{s,\circ}^\dagger \hat{a}_{s,\circ} \hat{q}_j \right. \\ &\quad \left. + \frac{\zeta_{p,j}}{2} (e^{-i\theta_d} \hat{a}_{s,\circ}^{\dagger 2} + e^{i\theta_d} \hat{a}_{s,\circ}^2) \hat{q}_j - F_j \hat{q}_j \right] + \chi \hat{q}_1 \hat{q}_2 \\ &\quad + i\varepsilon_{d,\circ} \sinh(r_d) (e^{-i\theta_d} \hat{a}_{s,\circ}^\dagger - e^{i\theta_d} \hat{a}_{s,\circ}) \\ &\quad + i\varepsilon_{d,\circ} \cosh(r_d) (\hat{a}_{s,\circ}^\dagger - \hat{a}_{s,\circ}),\end{aligned}\quad (3)$$

where $\omega_s = (\Delta_c - 2\Xi_d) \exp(2r_d)$ is the effective resonance frequency of the squeezed optical mode. $\zeta_{s,j} = g_j \cosh(2r_d)$ and $\zeta_{p,j} = g_j \sinh(2r_d)$ are the effective COM coupling strength for the j th mechanical mode induced by the radiation pressure and the parametric amplification, respectively. $F_j = g_j \sinh^2(r_d)$ denotes the strength of the constant mechanical driving force exerted on the j th mechanical mode, which is caused by the parametric amplification.

As discussed in the preceding studies [29, 56, 71, 72, 79], by adjusting the squeezing parameters with respect to the two-photon parametric driving field, the effective light-matter

interaction can be manipulated and enhanced in a controllable way. However, it is worth emphasizing that when the squeezed optical mode is coupled to a normal vacuum reservoir, the optical dissipation will be inevitably amplified in the meantime, thus leading to its quantum decoherence. To eliminate such optical dissipation induced by the intracavity squeezing, one can apply a broadband squeezed-vacuum reservoir that is phase-matched with the squeezed optical mode, i.e., the squeezing strength r_e and phase θ_e of this reservoir satisfying the relationships $r_e - r_d = 0$ and $\theta_e - \theta_d = \pm n\pi$ ($n = 1, 3, 5, \dots$). Note that the injection of this required broadband squeezed-vacuum reservoir has been reported through using an optical parametric amplifier [80]. Additionally, given that the two mechanical modes are coupled with two independent thermal reservoirs at same bath temperature T , the Born-Markovian master equation describing the dynamics of the whole system in the squeezing picture can be derived as [see Appendix B for more details]

$$\begin{aligned}\dot{\rho}_\circ &= i[\rho_\circ, \hat{H}_\circ] + \frac{\kappa}{2} \mathcal{D}[\hat{a}_{s,\circ}] \rho_\circ - \sum_{j=1,2} \left(i \frac{\gamma_{m,j}}{2} [\hat{q}_j, \{\hat{p}_j, \rho_\circ\}] \right. \\ &\quad \left. + \gamma_{m,j} \bar{n}_{m,j} [\hat{q}_j, [\hat{q}_j, \rho_\circ]] \right),\end{aligned}\quad (4)$$

where

$$\mathcal{D}[\hat{a}_{s,\circ}] \rho_\circ = 2\hat{a}_{s,\circ} \rho_\circ \hat{a}_{s,\circ}^\dagger - (\hat{a}_{s,\circ}^\dagger \hat{a}_{s,\circ} \rho_\circ + \rho_\circ \hat{a}_{s,\circ}^\dagger \hat{a}_{s,\circ}) \quad (5)$$

is the Lindblad operator, while $[\cdot, \cdot]$ and $\{\cdot, \cdot\}$ denote the commutator and anti-commutator, respectively. $\rho_\circ = S^\dagger(\eta_d) \rho_\circ S(\eta_d)$ is the density operator with respect to the CCW input case in the squeezing picture, with ρ_\circ the associated density operator in the original picture. $\gamma_{m,j}$ is the damping rate of the j th mechanical mode, and $\bar{n}_{m,j} = 1/[\exp(\omega_{m,j}/k_B T) - 1]$ is the corresponding mean thermal phonon excitation number, with k_B the Boltzmann constant.

For the CW input case, there is merely a coherent driving field with frequency $\omega_d/2$ applied to the waveguide. In this situation, the Hamiltonian of the whole system reads

$$\begin{aligned}\hat{H}_\circ &= \hat{H}_{\text{sys}} + \hat{H}_{\text{dr},\circ}, \\ \hat{H}_{\text{sys}} &= \Delta_c \hat{a}_\circ^\dagger \hat{a}_\circ + \sum_{j=1,2} \left[\frac{\omega_{m,j}}{2} (\hat{p}_j^2 + \hat{q}_j^2) - g_j \hat{a}_\circ^\dagger \hat{a}_\circ \hat{q}_j \right] \\ &\quad + \chi \hat{q}_1 \hat{q}_2, \\ \hat{H}_{\text{dr},\circ} &= i\varepsilon_{d,\circ} (\hat{a}_\circ^\dagger - \hat{a}_\circ),\end{aligned}\quad (6)$$

and the associated Born-Markovian master equation is given by [81]

$$\begin{aligned}\dot{\rho}_\circ &= i[\rho_\circ, \hat{H}_\circ] + \frac{\kappa}{2} \mathcal{D}[\hat{a}_\circ] \rho_\circ - \sum_{j=1,2} \left(i \frac{\gamma_{m,j}}{2} [\hat{q}_j, \{\hat{p}_j, \rho_\circ\}] \right. \\ &\quad \left. + \gamma_{m,j} \bar{n}_{m,j} [\hat{q}_j, [\hat{q}_j, \rho_\circ]] \right),\end{aligned}\quad (7)$$

where \hat{a}_\circ (\hat{a}_\circ^\dagger) is the annihilation (creation) operator of the CW mode, and ρ_\circ is the density operator with respect to the CW input case. Note that in the absence of the two-photon parametric driving field, the Bogoliubov transformation has

no influence on the system dynamics. Therefore, we apply a normal vacuum reservoir to the CW mode and analyze the dynamical evolution of this system in the original picture.

Comparing the two input scenarios, one can find that the primary distinction of their Hamiltonians and master equations lies in the injection of the two-photon parametric driving field and the squeezed-vacuum reservoir. It is seen that when setting $r_d = r_e = 0$ for the CCW input case, it will be equivalent to that of the CW case. In fact, because of this directional injection of quantum squeezing, the time-reversal symmetry of this system turns to be broken when interchanging the input direction of the coherent driving field, thus leading to the nonreciprocal features of this system. Hereafter, based on this characteristics, we merely show how to solve the system dynamics with respect to the CCW input case. For studying the CW input case, one can just set $r_d = r_e = 0$ for the CCW input case, and alter the index of the corresponding parameters and operators from \circlearrowleft to \circlearrowright .

For the CCW input case, due to the nonlinear COM interactions in Hamiltonian (3), the system dynamics is difficult to be directly solved. In order to deal with this problem, one can linearize the Hamiltonian by expanding each operator as a sum of its steady-state mean value and a small quantum fluctuation around it under the condition of strong coherent optical driving, i.e., $\hat{a}_{s,\circlearrowleft} = \bar{a}_{s,\circlearrowleft} + \delta\hat{a}_{s,\circlearrowleft}$, $\hat{q}_j = \bar{q}_j + \delta\hat{q}_j$, $\hat{p}_j = \bar{p}_j + \delta\hat{p}_j$. The steady-state mean values of the optical and mechanical modes can be derived by using the master equation (4), i.e.,

$$\begin{aligned} \bar{a}_{s,\circlearrowleft} &= -\frac{(i\Delta_s - \frac{\kappa}{2})A_1 + iA_2\beta_p}{(\Delta_s^2 + \frac{\kappa^2}{4}) - \beta_p^2}\varepsilon_{d,\circlearrowleft}, \\ \bar{q}_1 &= \frac{\omega_{m,2}B_1 - \chi B_2}{\omega_{m,1}\omega_{m,2} - \chi^2}, \quad \bar{p}_1 = 0, \\ \bar{q}_2 &= \frac{\omega_{m,1}B_2 - \chi B_1}{\omega_{m,1}\omega_{m,2} - \chi^2}, \quad \bar{p}_2 = 0, \end{aligned} \quad (8)$$

with

$$\begin{aligned} \alpha_s &= e^{-i\theta_d}\bar{a}_{s,\circlearrowleft}^{*2} + e^{i\theta_d}\bar{a}_{s,\circlearrowleft}^2, \\ \beta_s &= \zeta_{s,1}\bar{q}_1 + \zeta_{s,2}\bar{q}_2, \\ \beta_p &= \zeta_{p,1}\bar{q}_1 + \zeta_{p,2}\bar{q}_2, \\ \Delta_s &= \omega_s - \beta_s, \\ A_1 &= \cosh(r_d) + \sinh(r_d)e^{-i\theta_d}, \\ A_2 &= \cosh(r_d)e^{-i\theta_d} + \sinh(r_d), \\ B_1 &= \zeta_{s,1}|\bar{a}_{s,\circlearrowleft}|^2 - \frac{\zeta_{p,1}}{2}\alpha_s + F_1, \\ B_2 &= \zeta_{s,2}|\bar{a}_{s,\circlearrowleft}|^2 - \frac{\zeta_{p,2}}{2}\alpha_s + F_2. \end{aligned} \quad (9)$$

Equation (8) indicates that the field amplitude $\bar{a}_{s,\circlearrowleft}$ is not only dependent on the strength of the coherent driving field, but also relies on the squeezing strength and reference angle of the squeezed optical mode. This allows us to regulate the COM coupling strength and break the optical reciprocity of the system by adjusting the squeezing parameters. Moreover, it is also seen that the mean values of the mechanical displacement \bar{q}_j are coupled to each other by a factor of χ , which is

due to the phonon hopping process between the two mechanical modes.

Then, by substituting the expansions of the quantum operators into the Hamiltonian (3), one can directly derive the linearized Hamiltonian as

$$\begin{aligned} \hat{H}_{lin,\circlearrowleft} &= \Delta_s\hat{a}_{s,\circlearrowleft}^\dagger\hat{a}_{s,\circlearrowleft} + \sum_{j=1,2} \left[\frac{\omega_{m,j}}{2}(\hat{p}_j^2 + \hat{q}_j^2) \right. \\ &\quad \left. - (\Lambda_j\hat{a}_{s,\circlearrowleft}^\dagger + \Lambda_j^*\hat{a}_{s,\circlearrowleft})\hat{q}_j \right] + \chi\hat{q}_1\hat{q}_2, \end{aligned} \quad (10)$$

and the associated master equation as

$$\begin{aligned} \dot{\hat{\rho}}_\circlearrowleft &= i[\hat{\rho}_\circlearrowleft, \hat{H}_{lin,\circlearrowleft}] + \frac{\kappa}{2}\mathcal{D}[\hat{a}_{s,\circlearrowleft}]\hat{\rho}_\circlearrowleft - \sum_{j=1,2} \left(i\frac{\gamma_{m,j}}{2}[\hat{q}_j, \{\hat{p}_j, \hat{\rho}_\circlearrowleft\}] \right. \\ &\quad \left. + \gamma_{m,j}\bar{n}_{m,j}[\hat{q}_j, [\hat{q}_j, \hat{\rho}_\circlearrowleft]] \right), \end{aligned} \quad (11)$$

where

$$\Lambda_j = G_j \cosh(2r_d) - G_j^* \sinh(2r_d)e^{-i\theta_d} \quad (12)$$

is the effective COM coupling rate, with $G_j = g_j\bar{a}_{s,\circlearrowleft}$. For notational convenience, we have neglected the symbol “ δ ” in the expression of quantum fluctuation operators in Eqs. (10) and (11). We also emphasize that in the weak COM coupling regime, the steady-state mean value of the optical mode is much larger than those of the mechanical modes, i.e., $|\bar{a}_{s,\circlearrowleft}| \gg |\bar{q}_j|$. Under this condition, we have ignored the terms $\hat{a}_{s,\circlearrowleft}^2$ and $\hat{a}_{s,\circlearrowleft}^{\dagger 2}$ in Hamiltonian (10), whose coefficient β_p is dominated by \bar{q}_j . In the following discussions, for ensuring the validity of Hamiltonian (10), the system parameters have been strictly restricted to satisfy the condition of weak COM coupling.

Since the system dynamics is linearized now and the input noises for the optical and mechanical modes are Gaussian, the steady state of the system, independently of any initial state, could eventually evolve into a tripartite zero-mean Gaussian state, whose statistic is fully characterized by a 6×6 covariance matrix (CM) V with its matrix element

$$V_{kl} = \langle \psi_k \psi_l + \psi_l \psi_k \rangle / 2, \quad (k, l = 1, 2, \dots, 6). \quad (13)$$

Here $\psi = (\hat{X}, \hat{Y}, \hat{q}_1, \hat{p}_1, \hat{q}_2, \hat{p}_2)^T$ is the vector of optical and mechanical quadrature operators, with its components defined by

$$\hat{X} = \frac{1}{\sqrt{2}}(\hat{a}_{s,\circlearrowleft}^\dagger + \hat{a}_{s,\circlearrowleft}), \quad \hat{Y} = \frac{i}{\sqrt{2}}(\hat{a}_{s,\circlearrowleft}^\dagger - \hat{a}_{s,\circlearrowleft}). \quad (14)$$

Employing the master equation (11), one can obtain the dynamics of arbitrary quantum correlation between the optical and mechanical quadrature operators in the CM V . In terms of optical bosonic operator, we define the following quantum

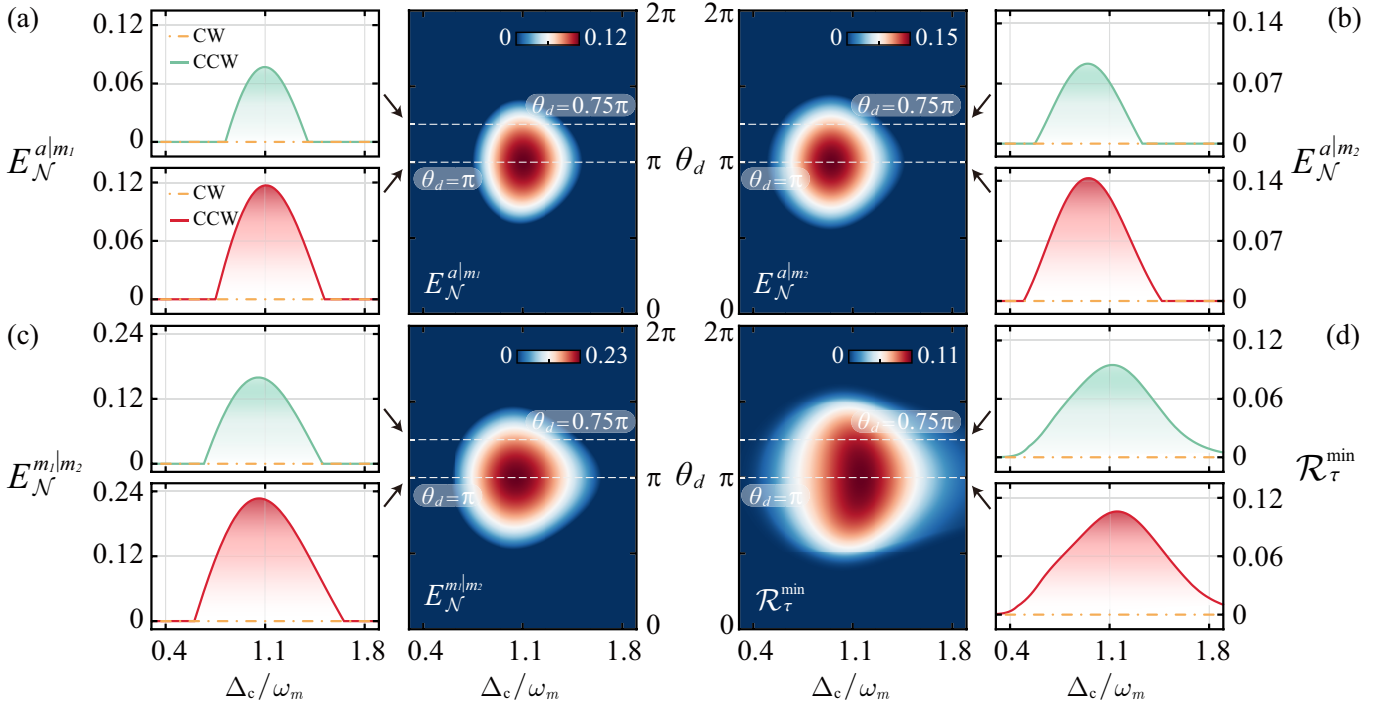


FIG. 2. Squeezing-induced nonreciprocal bipartite and tripartite entanglement. The logarithmic negativity $E_{\mathcal{N}}^{a|m_1}$ (a), $E_{\mathcal{N}}^{a|m_2}$ (b), $E_{\mathcal{N}}^{m_1|m_2}$ (c), and the minimum residual contangle $\mathcal{R}_{\tau}^{\min}$ (d) for opposite optical input directions are plotted as functions of the scaled optical detuning Δ_c/ω_m . The left panels of these figures show the bipartite and tripartite entanglement with respect to two specific squeezing reference angles of $\theta_d = 0.75\pi$ and π , respectively, with $r_d = 0.3$. The right panels show in detail the dependence of such entanglement on squeezing reference angle θ_d .

correlation functions

$$\begin{aligned}
 x_1 &= \langle \hat{a}_{s,\odot}^\dagger \hat{a}_{s,\odot} \rangle, & x_2 &= \langle \hat{a}_{s,\odot} \hat{a}_{s,\odot}^\dagger \rangle, & x_3 &= \langle \hat{q}_1 \hat{q}_1 \rangle, \\
 x_4 &= \langle \hat{p}_1 \hat{p}_1 \rangle, & x_5 &= \langle \hat{q}_2 \hat{q}_2 \rangle, & x_6 &= \langle \hat{p}_2 \hat{p}_2 \rangle, \\
 x_7 &= \langle \hat{a}_{s,\odot} \hat{a}_{s,\odot} \rangle, & x_8 &= \langle \hat{a}_{s,\odot}^\dagger \hat{a}_{s,\odot}^\dagger \rangle, & x_9 &= \langle \hat{q}_1 \hat{p}_1 \rangle, \\
 x_{10} &= \langle \hat{p}_1 \hat{q}_1 \rangle, & x_{11} &= \langle \hat{q}_2 \hat{p}_2 \rangle, & x_{12} &= \langle \hat{p}_2 \hat{q}_2 \rangle, \\
 x_{13} &= \langle \hat{a}_{s,\odot} \hat{q}_1 \rangle, & x_{14} &= \langle \hat{a}_{s,\odot}^\dagger \hat{q}_1 \rangle, & x_{15} &= \langle \hat{a}_{s,\odot} \hat{p}_1 \rangle, \\
 x_{16} &= \langle \hat{a}_{s,\odot}^\dagger \hat{p}_1 \rangle, & x_{17} &= \langle \hat{a}_{s,\odot} \hat{q}_2 \rangle, & x_{18} &= \langle \hat{a}_{s,\odot}^\dagger \hat{q}_2 \rangle, \\
 x_{19} &= \langle \hat{a}_{s,\odot} \hat{p}_2 \rangle, & x_{20} &= \langle \hat{a}_{s,\odot}^\dagger \hat{p}_2 \rangle, & x_{21} &= \langle \hat{q}_1 \hat{q}_2 \rangle, \\
 x_{22} &= \langle \hat{p}_1 \hat{p}_2 \rangle, & x_{23} &= \langle \hat{q}_1 \hat{p}_2 \rangle, & x_{24} &= \langle \hat{q}_2 \hat{p}_1 \rangle.
 \end{aligned} \tag{15}$$

By grouping together them in a vector, $X = (x_1, x_2, \dots, x_{24})^T$, one can obtain its time evolution equation as

$$\frac{d}{dt} X = M \cdot X + N, \tag{16}$$

where

$$\begin{aligned}
 N &= [0, \kappa, 0, 2\gamma_{m,1}\bar{n}_{m,1}, 0, 2\gamma_{m,2}\bar{n}_{m,2}, 0, 0, \\
 &0, 0, 0, 0, 0, 0, 0, 0, 0, 0, 0, 0, 0, 0]^T,
 \end{aligned} \tag{17}$$

is a vector involving the correlation functions for the input quantum noises. Here the exact expression for the coefficient matrix M and the detailed derivation process of the time

evolution equation (16) are too cumbersome, and, for convenience, we have reported them in Appendix C. Notably, by numerically solving Eq. (16) and using the relations between bosonic operators and quadrature operators, one can directly obtain the steady-state CM V .

Regarding the verification of bipartite and tripartite entanglement, we adopt the logarithmic negativity $E_{\mathcal{N}}$ and the minimum residual contangle $\mathcal{R}_{\tau}^{\min}$ as the quantitative entanglement measures, respectively, which are defined based on specifying the positivity of the partial transpose of the CM V . For continuous-variable (CV) bipartite Gaussian state, the logarithmic negativity $E_{\mathcal{N}}^{\mu|\nu}$ is defined as [15]

$$E_{\mathcal{N}}^{\mu|\nu} = \max [0, -\ln(2\eta_0^-)], \tag{18}$$

where $\eta_0^- \equiv 2^{-1/2} \{ \Sigma(V_{\mu\nu}) - [\Sigma(V_{\mu\nu})^2 - 4 \det V_{\mu\nu}]^{1/2} \}^{1/2}$, with $\Sigma(V_{\mu\nu}) \equiv \det \mathcal{A}_{\mu} + \det \mathcal{B}_{\nu} - 2 \det \mathcal{C}_{\mu\nu}$, is the minimum symplectic eigenvalue of the partial transpose of a reduced 4×4 CM $V_{\mu\nu}$. The reduced CM $V_{\mu\nu}$ contains the entries of V associated with the selected bipartition μ and ν , and it can be obtained by removing the rows and columns of the unwanted modes in V , whose 2×2 block form is given by

$$V_{\mu\nu} = \begin{pmatrix} \mathcal{A}_{\mu} & \mathcal{C}_{\mu\nu} \\ \mathcal{C}_{\mu\nu}^T & \mathcal{B}_{\nu} \end{pmatrix}. \tag{19}$$

Equation (18) quantifies how much the positivity of the partial transpose condition for separability is violated for the con-

sidered Gaussian states, and it is equivalent to Simon's necessary and sufficient entanglement nonpositive partial transpose criterion (or the related Peres-Horodecki criterion) [14]. The selected bipartition μ and ν gets entangled if and only if $\eta_0^- < 1/2$, where $E_{\mathcal{N}}$ has a nonzero value. To further confirm the presence and directionality of Gaussian steering between the two entangled bipartition μ and ν , we introduce an intuitive and computable quantification of quantum steerability [17], which is defined as

$$\begin{aligned} \mathcal{G}^{\mu \rightarrow \nu} &= \max \left[0, \frac{1}{2} \ln \frac{\det \mathcal{A}_{\mu}}{4 \det V_{\mu\nu}} \right], \\ \mathcal{G}^{\nu \rightarrow \mu} &= \max \left[0, \frac{1}{2} \ln \frac{\det \mathcal{B}_{\nu}}{4 \det V_{\mu\nu}} \right]. \end{aligned} \quad (20)$$

$\mathcal{G}^{\mu \rightarrow \nu} > 0$ ($\mathcal{G}^{\nu \rightarrow \mu} > 0$) implies that the bipartite Gaussian state characterized by CM $V_{\mu\nu}$ is steerable from mode μ (ν) to mode ν (μ) through Gaussian measurements on mode μ (ν), where a higher value of \mathcal{G} represents the stronger Gaussian steerability.

The minimum residual contangle, $\mathcal{R}_{\tau}^{\min}$, which provides a *bona fide* quantification of CV tripartite entanglement, is defined as [16]

$$\mathcal{R}_{\tau}^{\min} = \min_{(r,s,t)} [E_{\tau}^{r|st} - E_{\tau}^{r|s} - E_{\tau}^{r|t}], \quad (21)$$

where (r, s, t) denotes all the possible permutations of the three-mode indexes. $E_{\tau}^{\mu|\nu}$ is the contangle of subsystems of μ (μ contains one mode) and ν (ν contains one or two modes), which can be defined by a proper entanglement monotone, e.g., the squared logarithmic negativity. Based on Eq. (18), the one-mode-vs-one-mode contangle $E_{\tau}^{r|s}$ and $E_{\tau}^{r|t}$ can be directly obtained by employing its definition, namely, $E_{\tau}^{\mu|\nu} \equiv [E_{\mathcal{N}}^{\mu|\nu}]^2$. However, when calculating the one-mode-vs-two-modes contangle $E_{\tau}^{r|st}$, one must alter the basic definition of Eq. (18) by rewriting the definition of η_0^- as given by $\eta_0^- \equiv \min [\text{eig} |i\Omega_3 \tilde{V}_{r|st}|]$, where η_0^- becomes the minimum symplectic eigenvalue of the partial transpose of a 6×6 CM V , with $\Omega_3 = \bigoplus_{k=1}^3 i\sigma_y$ and σ_y the y-Pauli matrix. $\tilde{V}_{r|st}$ corresponds to the partial transpose of V , which connects to V with the relation of $\tilde{V}_{r|st} = P_{r|st} V P_{r|st}$, and $P_{r|st} = \text{diag}(1, -1, 1, 1, 1, 1)$ is the partial transposition matrix. In terms of $E_{\tau}^{s|rt}$ and $E_{\tau}^{t|sr}$, the corresponding partial transpose matrices are given by $P_{s|rt} = \text{diag}(1, 1, 1, -1, 1, 1)$ and $P_{t|sr} = \text{diag}(1, 1, 1, 1, 1, -1)$, respectively. In addition, according to the Coffman-Kundu-Wootters monogamy inequality for quantum entanglement, we also note that the residual contangle is required to satisfy the following monogamy condition, i.e., $E_{\tau}^{r|st} - E_{\tau}^{r|s} - E_{\tau}^{r|t} \geq 0$, which means that the bipartite entanglement between the partition r and the remaining two partitions st is never smaller than the sum of the $r|s$ and $r|t$ bipartite entanglements in the reduced states. As such, if there are nonzero values of the minimum residual contangle, i.e., $\mathcal{R}_{\tau}^{\min} > 0$, one can verify that the full tripartite entanglement is present for the CV system.

III. NONRECIPROCAL MANIPULATION OF QUANTUM ENTANGLEMENT AND EPR STEERING

Now we start to investigate the behaviors of quantum entanglement and EPR steering in regards to the coherent driving fields input from the CW and CCW direction in our proposed scheme. For this purpose, we evaluate the entanglement measures by numerically solving the dynamics of the steady-state CM V (16) within the following parameters: $\kappa/2\pi = 1750$ Hz, $\omega_m/2\pi = 1945$ Hz, $\gamma_m/2\pi = 195$ Hz, $g_1/2\pi = 214$ Hz, $g_2/2\pi = 321$ Hz, $\chi/2\pi = 292$ Hz, $\bar{n}_m = 0.9$, $\theta_e = 0$, which is partially chosen from a recent experiment [76]. Note that, for simplicity and without loss of generality, we have supposed that the two mechanical modes are identical, i.e., $\omega_{m,1} = \omega_{m,2} = \omega_m$, $\gamma_{m,1} = \gamma_{m,2} = \gamma_m$, $\bar{n}_{m,1} = \bar{n}_{m,2} = \bar{n}_m$, while their COM coupling strength are asymmetric, i.e., $g_2/g_1 = 1.5$. This condition is convenient for producing quantum entanglement and EPR steering.

We first present how to achieve nonreciprocal bipartite and tripartite entanglement by leveraging a directional two-photon parametric driving field. Figure 2 shows the logarithmic negativity $E_{\mathcal{N}}^{a|m_1}$, $E_{\mathcal{N}}^{a|m_2}$, $E_{\mathcal{N}}^{m_1|m_2}$ and the minimum residual contangle $\mathcal{R}_{\tau}^{\min}$ for opposite optical input directions as functions of the scaled optical detuning Δ_c/ω_m . Here $E_{\mathcal{N}}^{a|m_j}$ corresponds to the logarithmic negativity of the bipartition of the optical mode and the j th mechanical mode, while $E_{\mathcal{N}}^{m_1|m_2}$ corresponds to that of the bipartition of the two mechanical modes. In terms of the CW input case, as shown in the left panels of Figs. 2(a)-2(d), it is seen that in the absence of a two-photon parametric driving field, i.e., $r_d = r_e = 0$, all of the logarithmic negativity $E_{\mathcal{N}}^{a|m_1}$, $E_{\mathcal{N}}^{a|m_2}$, $E_{\mathcal{N}}^{m_1|m_2}$ and the minimum residual contangle $\mathcal{R}_{\tau}^{\min}$ are null within the considered optical detuning (yellow dashed curve), indicating that there is no bipartite and tripartite entanglement in this system when only applying a coherent driving field. In contrast, for the CCW input case, it is seen that in the presence of a two-photon parametric driving field (with, e.g., squeezing strength $r_d = r_e = 0.3$), the profiles of $E_{\mathcal{N}}^{a|m_1}$, $E_{\mathcal{N}}^{a|m_2}$, $E_{\mathcal{N}}^{m_1|m_2}$ and $\mathcal{R}_{\tau}^{\min}$ are all characterized by a sharp peak around the optical detuning at COM resonance $\Delta_c/\omega_m \sim 1$. Meanwhile, as shown in the right panels of Figs. 2(a)-2(d), the bipartite and tripartite entanglement are also sensitive to the variation of the squeezing reference angle θ_d , which all reach their maximum values at an optimal phase angle of $\theta_d = \pi$. This result is consistent with that of the previous study [29], in which it reveals that the maximum COM interaction and the minimum optical noise are both obtained under the phase-matched condition with $r_e - r_d = 0$ and $\theta_e - \theta_d = \pm n\pi$ ($n = 1, 3, 5, \dots$), resulting in an enhanced COM entanglement. By comparing these results of the CW and CCW input cases, one can intuitively find that by applying a directional two-photon parametric driving field with a proper squeezing phase, the nonreciprocal generation and manipulation of bipartite and tripartite entanglement can be achieved, namely, such entanglement can emerge only for one specific optical input direction when reversing the coherent driving field. Physically, the mechanism behind these results is that the directional input of a two-photon parametric

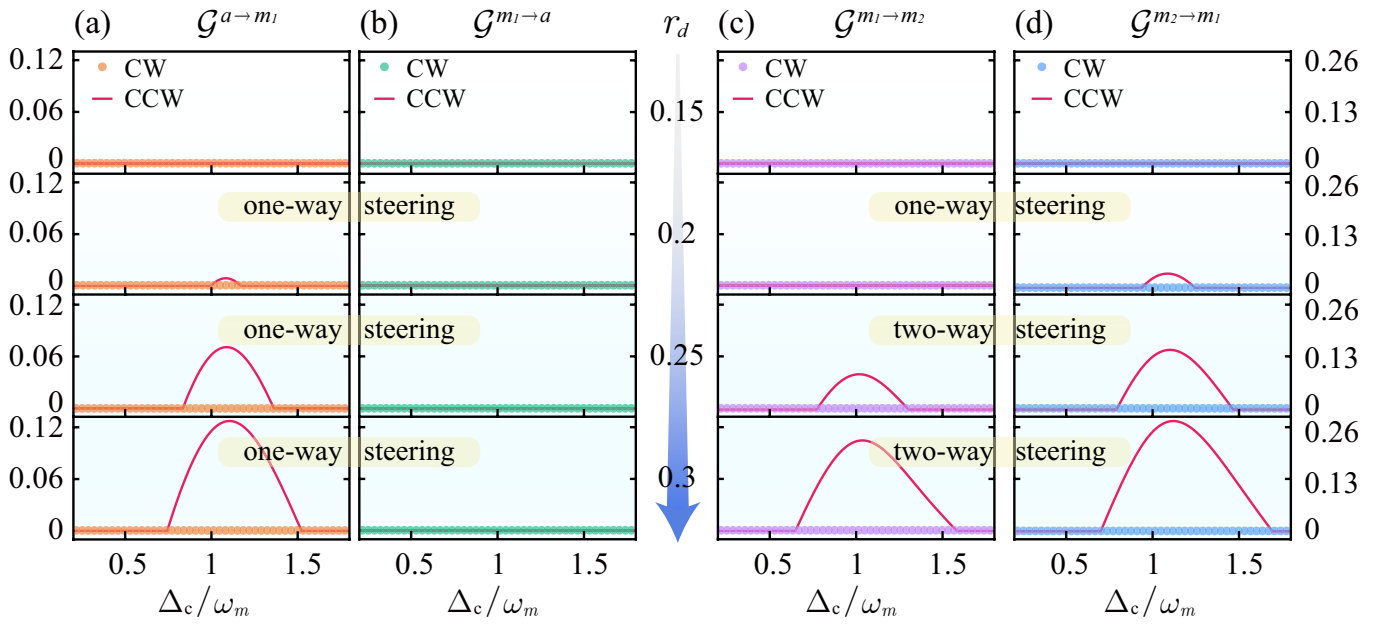


FIG. 3. Squeezing-induced nonreciprocal EPR steering. The quantum steerability $\mathcal{G}^{a \rightarrow m_1}$ (a), $\mathcal{G}^{m_1 \rightarrow a}$ (b), $\mathcal{G}^{m_1 \rightarrow m_2}$ (c), and $\mathcal{G}^{m_2 \rightarrow m_1}$ (d) for opposite optical input directions are plotted as functions of the scaled optical detuning Δ_c/ω_m under different squeezing parameter r_d . With the increase of r_d , EPR steering can be stepwise driven from no-way regime, one-way regime to two-way regime for the CCW input case but not for the CW input case, indicating the achievement of nonreciprocal EPR steering.

driving field allows one to regulate the effective COM coupling strength for the CW and CCW modes in an asymmetric way, by which one can break the time-reversal symmetry of this system. This feature of the system provides a flexible tool to tailor the parameter condition for entanglement generation based on its optical input direction. Consequently, when preparing the system under a directional entanglement generation condition, nonreciprocal bipartite and tripartite entanglement will be achieved.

After having established nonreciprocal entanglement, we further show how to manipulate the directionality of EPR steering. In Fig. 3, we plot the quantum steerability $\mathcal{G}^{a \rightarrow m_1}$, $\mathcal{G}^{m_1 \rightarrow a}$, $\mathcal{G}^{m_1 \rightarrow m_2}$ and $\mathcal{G}^{m_2 \rightarrow m_1}$ as a function of the scaled optical detuning Δ_c/ω_m under different squeezing parameter r_d . Figures 3(a) and 3(b) show the EPR steering between the optical mode and the mechanical mode for opposite optical input directions. For the CW input case ($r_d = r_e = 0$), since the optomechanical entanglement is absent, EPR steering, as a stronger quantum correlation, can also not be produced, where $\mathcal{G}^{a \rightarrow m_1}$ and $\mathcal{G}^{m_1 \rightarrow a}$ always keep zero with the variation of the controlling parameters [see scattered dotted curve in Figs. 3(a) and 3(b)]. For the CCW input case, due to the introduction of the squeezed optical mode and the emergence of the optomechanical entanglement, one can create an asymmetric and directional EPR steering by adjusting the squeezing parameters. For instance, it is seen that although when choosing $\theta_d = \pi$ and some small values of r_d , such as $r_d = 0.15$, the EPR steering still does not exist for both $a \rightarrow m_1$ and $m_1 \rightarrow a$, i.e., $\mathcal{G}^{a \rightarrow m_1} = \mathcal{G}^{m_1 \rightarrow a} = 0$ [solid curve in the top panels of Figs. 3(a) and 3(b)]. However, when the squeezing strength r_d is continued to be raised, the

value of $\mathcal{G}^{a \rightarrow m_1}$ will become nonzero and monotonically increase, resulting in an asymmetric one-way EPR steering with $\mathcal{G}^{a \rightarrow m_1} > 0$ and $\mathcal{G}^{m_1 \rightarrow a} = 0$. Moreover, we also show the EPR steering between the two mechanical modes for opposite optical input directions in Figs. 3(c) and 3(d). For the CW input case, there is no EPR steering for both $m_1 \rightarrow m_2$ and $m_2 \rightarrow m_1$, i.e., $\mathcal{G}^{m_1 \rightarrow m_2} = \mathcal{G}^{m_2 \rightarrow m_1} = 0$ [see scattered dotted curve in Figs. 3(c) and 3(d)], which is similar to the case discussed above for the optomechanical bipartition. For the CCW input case, accompanied by the occurrence of entanglement, we can get rich properties of EPR steering, where the overall state's asymmetry is stepwise driven through the no-way regime ($\mathcal{G}^{m_1 \rightarrow m_2} = \mathcal{G}^{m_2 \rightarrow m_1} = 0$), one-way regime ($\mathcal{G}^{m_1 \rightarrow m_2} = 0$ but $\mathcal{G}^{m_2 \rightarrow m_1} > 0$), and finally two-way regime ($\mathcal{G}^{m_1 \rightarrow m_2} > 0$ and $\mathcal{G}^{m_2 \rightarrow m_1} > 0$) with the increase of the squeezing strength r_d . From the above discussions, it is found that EPR steering can be generated and manipulated only for the CCW input case but not for the CW input case, which implies the achievement of nonreciprocal EPR steering. These results can be understood as follows: The proposed three-mode COM system has a bilinear cyclic coupling among the optical mode and the two mechanical modes. For an arbitrary bipartition μ and ν , apart from their direct interaction, there is also an indirect interaction induced by their coupling to the third intermediate mode. Both direct and indirect interaction paths can generate EPR steering between μ and ν , whose superposition may induce quantum interference effect that depends on the relative phase and strength of the two interaction paths. As discussed previously, by applying a directional two-photon parametric driving field, one can manipulate the COM coupling strength in an asymmetric way. In this case,

the relative strength of the two interaction paths for any bipartition of this system is influenced, based on which the manipulation of the directionality of EPR steering can be achieved by tuning the squeezing strength.

IV. CONCLUSION

In summary, we have presented how to generate and manipulate squeezing-induced nonreciprocal quantum entanglement and asymmetric EPR steering in a three-mode COM system consisting of a bottle WGM resonator, an optical waveguide, and a tapered glass-fiber nanospike. The WGM resonator supports two counterpropagating optical modes, which are uncoupled and degenerate. The coherent driving field from the waveguide is coupled into and out of the WGM resonator via evanescent coupling. Moreover, when placing the nanospike close to the WGM resonator, it excites two mechanical modes due to the COM interaction induced by the WGM evanescent field, whose vibrating directions are orthogonal or parallel to the resonator surface. First, we show that when applying an additional two-photon parametric driving field for one specific input direction of the WGM resonator with a phase-matched squeezed vacuum reservoir, one can introduce a squeezed optical mode and an enhanced COM interaction in this input direction. This directional injection of quantum squeezing breaks the time-reversal symmetry of the system, and it allows one to tailor the parameter condition for entanglement generation with respect to its optical input direction, which is essential for achieving quantum nonreciprocity. Second, based on this unique feature of the system, we find that when reversing the input direction of the coherent driving field, quantum entanglement and the associated EPR steering is regulated in an asymmetric way, whereby a controllable nonreciprocal generation and manipulation of quantum entanglement and EPR steering is achieved. More interestingly, it is also found that by properly tuning the squeezing parameters, the directionality of EPR steering can be well controlled. According to this, we further show that with the increase of the squeezing strength, EPR steering can be stepwise driven from no-way regime, one-way regime to two-way regime. These results might open up new perspectives for the experimental generation and application of nonreciprocal bipartite and tripartite entanglement and asymmetric EPR steering as a precious resource for a variety of nascent quantum technologies ranging from one-sided device-independent quantum key distribution to no-cloning quantum teleportation [9–13].

V. ACKNOWLEDGMENT

H.J. is supported by the National Natural Science Foundation of China (NSFC, Grant No. 11935006, 12421005), the National Key R&D Program of China (Grants No. 2024YFE0102400), the Hunan Provincial Major Sci-Tech Program (Grant No. 2023ZJ1010), and the Science and Technology Innovation Program of Hunan Province (Grant No. 2020RC4047). L.-M.K. is supported by the NSFC

(Grants No. 12247105, 11935006, 12175060 and 12421005), the Hunan Provincial Major Sci-Tech Program (Grant No. 2023ZJ1010), and the Henan Science and Technology Major Project (Grant No. 241100210400). Y.-F.J. is supported by the NSFC (Grant No. 12405029). D.-Y.W. is supported by the NSFC (Grant No. 12204424) and the China Postdoctoral Science Foundation (Grant No. 2022M722889). L.T. is supported by the NSFC (Grant No. 12305023) and the Sichuan Science and Technology Program (Grant No. 2024NSFSC1353). Y.W. is supported by the NSFC (Grant No. 12205256) and the Henan Provincial Science and Technology Research Project (Grant No. 232102221001). W.-S.B. is supported by the Henan Science and Technology Major Project of the Department of Science & Technology of Henan Province (Grant No. 241100210400).

Appendix A: Derivation of the effective Hamiltonian

To diagonalize the optical mode of Hamiltonian (1), one can perform a unitary Bogoliubov transformation with $S(\eta_d) = \exp[(-\eta_d \hat{a}_{s,\circ}^{\dagger 2} + \eta_d^* \hat{a}_{s,\circ}^2)/2]$, where $\eta_d = r_d e^{-i\theta_d}$ is a complex squeezing parameter with r_d the squeezing strength and θ_d the squeezing reference angle. By implementing this Bogoliubov transformation, a squeezed optical mode is introduced and the system Hamiltonian (1) becomes

$$\begin{aligned}
\hat{H}_{\circ} &= S^{\dagger}(\eta_d) \hat{H}_{\circ} S(\eta_d) \\
&= \frac{\omega_{m,1}}{2} (\hat{p}_1^2 + \hat{q}_1^2) + \frac{\omega_{m,2}}{2} (\hat{p}_2^2 + \hat{q}_2^2) + \chi \hat{q}_1 \hat{q}_2 \\
&\quad + [\Delta_c \cosh(2r_d) - 2\Xi_d \sinh(2r_d)] \hat{a}_{s,\circ}^{\dagger} \hat{a}_{s,\circ} \\
&\quad + \left[\Xi_d \cosh(2r_d) - \frac{\Delta_c}{2} \sinh(2r_d) \right] e^{-i\theta_d} \hat{a}_{s,\circ}^{\dagger 2} \\
&\quad + \left[\Xi_d \cosh(2r_d) - \frac{\Delta_c}{2} \sinh(2r_d) \right] e^{i\theta_d} \hat{a}_{s,\circ}^2 \\
&\quad - g_1 \cosh(2r_d) \hat{a}_{s,\circ}^{\dagger} \hat{a}_{s,\circ} \hat{q}_1 - g_2 \cosh(2r_d) \hat{a}_{s,\circ}^{\dagger} \hat{a}_{s,\circ} \hat{q}_2 \\
&\quad + \frac{1}{2} g_1 \sinh(2r_d) (e^{-i\theta_d} \hat{a}_{s,\circ}^{\dagger 2} + e^{i\theta_d} \hat{a}_{s,\circ}^2) \hat{q}_1 \\
&\quad + \frac{1}{2} g_2 \sinh(2r_d) (e^{-i\theta_d} \hat{a}_{s,\circ}^{\dagger 2} + e^{i\theta_d} \hat{a}_{s,\circ}^2) \hat{q}_2 \\
&\quad - g_1 \sinh^2(r_d) \hat{q}_1 - g_2 \sinh^2(r_d) \hat{q}_2 \\
&\quad + i\varepsilon_{d,\circ} \cosh(r_d) (\hat{a}_{s,\circ}^{\dagger} - \hat{a}_{s,\circ}) \\
&\quad + i\varepsilon_{d,\circ} \sinh(r_d) (e^{-i\theta_d} \hat{a}_{s,\circ}^{\dagger} - e^{i\theta_d} \hat{a}_{s,\circ}) \\
&\quad + \Delta_c \sinh^2(r_d) - \Xi_d \sinh(2r_d). \tag{A1}
\end{aligned}$$

By setting the coefficients of the quadratic terms $\hat{a}_{s,\circ}^{\dagger 2}$ and $\hat{a}_{s,\circ}^2$ to be zero, i.e.,

$$\Delta_c \cosh(2r_d) - 2\Xi_d \sinh(2r_d) = 0, \tag{A2}$$

we have $r_d = (1/4) \ln[(\Delta_c + 2\Xi_d)/(\Delta_c - 2\Xi_d)]$. Correspondingly, the effective Hamiltonian of the system is obtained as

$$\begin{aligned} \hat{H}_\circ &= \omega_s \hat{a}_{s,\circ}^\dagger \hat{a}_{s,\circ} + \frac{\omega_{m,1}}{2} (\hat{p}_1^2 + \hat{q}_1^2) + \frac{\omega_{m,2}}{2} (\hat{p}_2^2 + \hat{q}_2^2) \\ &\quad - \zeta_{s,1} \hat{a}_{s,\circ}^\dagger \hat{a}_{s,\circ} \hat{q}_1 + \frac{\zeta_{p,1}}{2} (e^{-i\theta_d} \hat{a}_{s,\circ}^{\dagger 2} + e^{i\theta_d} \hat{a}_{s,\circ}^2) \hat{q}_1 \\ &\quad - \zeta_{s,2} \hat{a}_{s,\circ}^\dagger \hat{a}_{s,\circ} \hat{q}_2 + \frac{\zeta_{p,2}}{2} (e^{-i\theta_d} \hat{a}_{s,\circ}^{\dagger 2} + e^{i\theta_d} \hat{a}_{s,\circ}^2) \hat{q}_2 \\ &\quad - F_1 \hat{q}_1 - F_2 \hat{q}_2 + \chi \hat{q}_1 \hat{q}_2 + i\varepsilon_{d,\circ} \cosh(r_d) (\hat{a}_{s,\circ}^\dagger - \hat{a}_{s,\circ}) \\ &\quad + i\varepsilon_{d,\circ} \sinh(r_d) (e^{-i\theta_d} \hat{a}_{s,\circ}^\dagger - e^{i\theta_d} \hat{a}_{s,\circ}) + C, \quad (\text{A3}) \end{aligned}$$

where

$$\begin{aligned} \omega_s &= \Delta_c \cosh(2r_d) - 2\Xi_d \sinh(2r_d) = (\Delta_c - 2\Xi_d) \exp(2r_d), \\ \zeta_{s,j} &= \frac{g_j \Delta_c}{\sqrt{\Delta_c^2 - 4\Xi_d^2}} = g_j \cosh(2r_d), \\ \zeta_{p,j} &= \frac{2g_j \Xi_d}{\sqrt{\Delta_c^2 - 4\Xi_d^2}} = g_j \sinh(2r_d), \\ F_j &= g_j \sinh^2(r_d), \quad C = \Delta_c \sinh^2(r_d) - \Xi_d \sinh(2r_d). \quad (\text{A4}) \end{aligned}$$

Appendix B: Derivation of the effective master equation under phase-matched condition

For the CCW input case, to eliminate the optical dissipation induced by the intracavity squeezing, we consider the injection of a broadband squeezed optical field in this direction, which can act as a squeezed-vacuum reservoir. We assume the squeezed optical field, with squeezing strength r_e and reference phase angle θ_e , is around the central frequency ω_c . Besides, the two mechanical modes are assumed to be coupled with two independent thermal reservoirs at the same bath temperature T . Then, including the dissipations of the optical and mechanical modes, the dynamics of the total system in the original picture is governed by the Born-Markovian master equation [81]

$$\begin{aligned} \dot{\rho}_\circ &= i[\rho_\circ, \hat{H}_\circ] + \frac{\kappa}{2} (N_e + 1) \mathcal{D}[\hat{a}_\circ] \rho_\circ + \frac{\kappa}{2} N_e \mathcal{D}[\hat{a}_\circ^\dagger] \rho_\circ \\ &\quad - \frac{\kappa}{2} M_e \mathcal{G}[\hat{a}_\circ] \rho_\circ - \frac{\kappa}{2} M_e^* \mathcal{G}[\hat{a}_\circ^\dagger] \rho_\circ \\ &\quad - \sum_{j=1,2} \left(i \frac{\gamma_{m,j}}{2} [\hat{q}_j, \{\hat{p}_j, \rho_\circ\}] + \gamma_{m,j} \bar{n}_{m,j} [\hat{q}_j, [\hat{q}_j, \rho_\circ]] \right), \quad (\text{B1}) \end{aligned}$$

where

$$\begin{aligned} \mathcal{D}[\hat{a}_\circ] \rho_\circ &= 2\hat{a}_\circ \rho_\circ \hat{a}_\circ^\dagger - (\hat{a}_\circ^\dagger \hat{a}_\circ \rho_\circ + \rho_\circ \hat{a}_\circ^\dagger \hat{a}_\circ), \\ \mathcal{G}[\hat{a}_\circ] \rho_\circ &= 2\hat{a}_\circ \rho_\circ \hat{a}_\circ - (\hat{a}_\circ \hat{a}_\circ \rho_\circ + \rho_\circ \hat{a}_\circ \hat{a}_\circ), \quad (\text{B2}) \end{aligned}$$

and κ ($\gamma_{m,j}$) is the optical (mechanical) decay rate. $\bar{n}_{m,j} = 1/[\exp(\omega_{m,j}/k_B T) - 1]$ is the thermal phonon number, while $N_e = \sinh^2(r_e)$ and $M_e = \cosh(r_e) \sinh(r_e) e^{i\theta_e}$ describe the dissipation and the two-photon correlation of the cavity field caused by the squeezed-vacuum reservoir, respectively.

By introducing the Bogoliubov transformation in Eq. (2), the Lindblad operators becomes

$$\begin{aligned} &S^\dagger(\eta_d) \mathcal{D}[\hat{a}_\circ] \rho_\circ S(\eta_d) \\ &= 2 \cosh^2(r_d) \hat{a}_{s,\circ} \tilde{\rho}_\circ \hat{a}_{s,\circ}^\dagger + 2 \sinh^2(r_d) \hat{a}_{s,\circ}^\dagger \tilde{\rho}_\circ \hat{a}_{s,\circ} \\ &\quad - \sinh(2r_d) (e^{-i\theta_d} \hat{a}_{s,\circ}^\dagger \tilde{\rho}_\circ \hat{a}_{s,\circ}^\dagger + e^{i\theta_d} \hat{a}_{s,\circ} \tilde{\rho}_\circ \hat{a}_{s,\circ}) \\ &\quad - \left[\cosh^2(r_d) \hat{a}_{s,\circ}^\dagger \hat{a}_{s,\circ} \tilde{\rho}_\circ + \sinh^2(r_d) \hat{a}_{s,\circ} \hat{a}_{s,\circ}^\dagger \tilde{\rho}_\circ \right. \\ &\quad \left. - \sinh(r_d) \cosh(r_d) (e^{-i\theta_d} \hat{a}_{s,\circ}^\dagger \hat{a}_{s,\circ}^\dagger \tilde{\rho}_\circ + e^{i\theta_d} \hat{a}_{s,\circ} \hat{a}_{s,\circ} \tilde{\rho}_\circ) \right] \\ &\quad - \left[\cosh^2(r_d) \tilde{\rho}_\circ \hat{a}_{s,\circ}^\dagger \hat{a}_{s,\circ} + \sinh^2(r_d) \tilde{\rho}_\circ \hat{a}_{s,\circ} \hat{a}_{s,\circ}^\dagger \right. \\ &\quad \left. - \sinh(r_d) \cosh(r_d) (e^{-i\theta_d} \tilde{\rho}_\circ \hat{a}_{s,\circ}^\dagger \hat{a}_{s,\circ}^\dagger + e^{i\theta_d} \tilde{\rho}_\circ \hat{a}_{s,\circ} \hat{a}_{s,\circ}) \right], \\ &S^\dagger(\eta_d) \mathcal{G}[\hat{a}_\circ] \rho_\circ S(\eta_d) \\ &= 2e^{-2i\theta_d} \sinh^2(r_d) \hat{a}_{s,\circ}^\dagger \tilde{\rho}_\circ \hat{a}_{s,\circ}^\dagger + 2 \cosh^2(r_d) \hat{a}_{s,\circ} \tilde{\rho}_\circ \hat{a}_{s,\circ} \\ &\quad - e^{-i\theta_d} \sinh(2r_d) (\hat{a}_{s,\circ}^\dagger \tilde{\rho}_\circ \hat{a}_{s,\circ} + \hat{a}_{s,\circ} \tilde{\rho}_\circ \hat{a}_{s,\circ}^\dagger) \\ &\quad - \left[e^{-2i\theta_d} \sinh^2(r_d) \hat{a}_{s,\circ}^\dagger \hat{a}_{s,\circ}^\dagger \tilde{\rho}_\circ + \cosh^2(r_d) \hat{a}_{s,\circ} \hat{a}_{s,\circ} \tilde{\rho}_\circ \right. \\ &\quad \left. - e^{-i\theta_d} \sinh(r_d) \cosh(r_d) (\hat{a}_{s,\circ}^\dagger \hat{a}_{s,\circ} \tilde{\rho}_\circ + \hat{a}_{s,\circ} \hat{a}_{s,\circ}^\dagger \tilde{\rho}_\circ) \right] \\ &\quad - \left[e^{-2i\theta_d} \sinh^2(r_d) \tilde{\rho}_\circ \hat{a}_{s,\circ}^\dagger \hat{a}_{s,\circ}^\dagger + \cosh^2(r_d) \tilde{\rho}_\circ \hat{a}_{s,\circ} \hat{a}_{s,\circ} \right. \\ &\quad \left. - e^{-i\theta_d} \sinh(r_d) \cosh(r_d) (\tilde{\rho}_\circ \hat{a}_{s,\circ}^\dagger \hat{a}_{s,\circ} + \tilde{\rho}_\circ \hat{a}_{s,\circ} \hat{a}_{s,\circ}^\dagger) \right]. \quad (\text{B3}) \end{aligned}$$

In this case, the effective Born-Markovian master equation could be rewritten as

$$\begin{aligned} \dot{\tilde{\rho}}_\circ &= S^\dagger(\eta_d) \dot{\rho}_\circ S(\eta_d) \\ &= i[\tilde{\rho}_\circ, \hat{H}_\circ] + \frac{\kappa}{2} (N_s + 1) \mathcal{D}[\hat{a}_\circ] \tilde{\rho}_\circ + \frac{\kappa}{2} N_s \mathcal{D}[\hat{a}_\circ^\dagger] \tilde{\rho}_\circ \\ &\quad - \frac{\kappa}{2} M_s \mathcal{G}[\hat{a}_\circ] \tilde{\rho}_\circ - \frac{\kappa}{2} M_s^* \mathcal{G}[\hat{a}_\circ^\dagger] \tilde{\rho}_\circ \\ &\quad - \sum_{j=1,2} \left(i \frac{\gamma_{m,j}}{2} [\hat{q}_j, \{\hat{p}_j, \tilde{\rho}_\circ\}] + \gamma_{m,j} \bar{n}_{m,j} [\hat{q}_j, [\hat{q}_j, \tilde{\rho}_\circ]] \right), \quad (\text{B4}) \end{aligned}$$

where

$$\begin{aligned} N_s &= \sinh^2(r_d) \cosh^2(r_e) + \cosh^2(r_d) \sinh^2(r_e) \\ &\quad + \frac{1}{2} \cos(\theta_e - \theta_d) \sinh(2r_d) \sinh(2r_e), \\ M_s &= e^{i\theta_d} [\cosh(r_d) \cosh(r_e) + e^{-i(\theta_e - \theta_d)} \sinh(r_d) \sinh(r_e)] \\ &\quad \times [\sinh(r_d) \cosh(r_e) + e^{i(\theta_e - \theta_d)} \cosh(r_d) \sinh(r_e)]. \quad (\text{B5}) \end{aligned}$$

Here N_s and M_s denote the effective thermal noise and two-photon-correlation strength, respectively, which can be simplified in case of $r_d = r_e = r$, i.e.,

$$\begin{aligned} N_s &= \frac{1}{2} \sinh^2(2r) [1 + \cos(\theta_e - \theta_d)], \\ M_s &= \frac{1}{2} e^{i\theta_d} \sinh(2r) [1 + e^{i(\theta_e - \theta_d)}] \\ &\quad \times [\cosh^2(r) + e^{-i(\theta_e - \theta_d)} \sinh^2(r)]. \quad (\text{B6}) \end{aligned}$$

Obviously, the thermal noise N_s and the two-photon-correlation strength M_s can be completely eliminated by choosing $r_p = r_e$ and $\theta_e - \theta_d = \pm n\pi$ ($n = 1, 3, 5, \dots$), i.e., $N_s = M_s = 0$. As discussed in Ref. [], the reservoir of the original optical mode is squeezed along the axis with angle $\frac{\theta_e}{2}$. In the basis of the squeezed optical mode $\hat{a}_{s,\circ}$, this effect can be canceled by the squeezing (along axis $\frac{\theta_d}{2}$) induced by the parametric amplification of \hat{a}_\circ , when $r_p = r_e$ and $\theta_e + \theta_d = \pm n\pi$ ($n = 1, 3, 5, \dots$), yielding the phase-matched condition. This means the squeezed-vacuum reservoir of \hat{a}_\circ corresponds to an effective vacuum reservoir of $\hat{a}_{s,\circ}$ under the phase-matched condition. In this case, the effective Born-Markovian master equation is derived as

$$\begin{aligned} \dot{\hat{\rho}}_\circ = & i[\hat{\rho}_\circ, \hat{H}_\circ] + \frac{\kappa}{2}\mathcal{D}[\hat{a}_{s,\circ}]\hat{\rho}_\circ - \sum_{j=1,2} \left(i\frac{\gamma_{m,j}}{2}[\hat{q}_j, \{\hat{p}_j, \hat{\rho}_\circ\}] \right. \\ & \left. + \gamma_{m,j}\bar{n}_{m,j}[\hat{q}_j, [\hat{q}_j, \hat{\rho}_\circ]] \right), \end{aligned} \quad (\text{B7})$$

where

$$\mathcal{D}[\hat{a}_{s,\circ}]\hat{\rho}_\circ = 2\hat{a}_{s,\circ}\hat{\rho}_\circ\hat{a}_{s,\circ}^\dagger - (\hat{a}_{s,\circ}^\dagger\hat{a}_{s,\circ}\hat{\rho}_\circ + \hat{\rho}_\circ\hat{a}_{s,\circ}^\dagger\hat{a}_{s,\circ}) \quad (\text{B8})$$

are the effective Lindblad operators, while $[\cdot, \cdot]$ and $\{\cdot, \cdot\}$ denote the commutator and anti-commutator, respectively.

Appendix C: Derivation of the dynamics of the quantum correlation function

By employing the linearized effective master equation (11), the dynamics of the quantum correlation function in the vector X can be derived as

$$\dot{x}_1 = -\kappa x_1 + i\Lambda_1 x_{14} - i\Lambda_1^* x_{13} + i\Lambda_2 x_{18} - i\Lambda_2^* x_{17}, \quad (\text{C1})$$

$$\dot{x}_2 = -\kappa x_2 + i\Lambda_1 x_{14} - i\Lambda_1^* x_{13} + i\Lambda_2 x_{18} - i\Lambda_2^* x_{17} + \kappa, \quad (\text{C2})$$

$$\dot{x}_3 = 2\omega_{m,1} x_9 + 2\omega_{m,1} x_{10}, \quad (\text{C3})$$

$$\begin{aligned} \dot{x}_4 = & -2\gamma_{m,1} x_4 - 2\omega_{m,1} x_9 - 2\omega_{m,1} x_{10} + 2\Lambda_1 x_{16} \\ & + 2\Lambda_1^* x_{15} - 2\chi x_{24} + 2\gamma_{m,1} \bar{n}_{m,1}, \end{aligned} \quad (\text{C4})$$

$$\dot{x}_5 = 2\omega_{m,2} x_{11} + 2\omega_{m,2} x_{12}, \quad (\text{C5})$$

$$\begin{aligned} \dot{x}_6 = & -2\gamma_{m,2} x_6 - 2\omega_{m,2} x_{11} - 2\omega_{m,2} x_{12} + 2\Lambda_2 x_{20} \\ & + 2\Lambda_2^* x_{19} - 2\chi x_{23} + 2\gamma_{m,2} \bar{n}_{m,2}, \end{aligned} \quad (\text{C6})$$

$$\dot{x}_7 = -(2i\Delta_s + \kappa)x_7 + 2i\Lambda_1 x_{13} + 2i\Lambda_2 x_{17}, \quad (\text{C7})$$

$$\dot{x}_8 = (2i\Delta_s - \kappa)x_8 - 2i\Lambda_1^* x_{14} - 2i\Lambda_2^* x_{18}, \quad (\text{C8})$$

$$\begin{aligned} \dot{x}_9 = & -\frac{\gamma_{m,1}}{2}x_9 - \frac{\gamma_{m,1}}{2}x_{10} + \omega_{m,1}x_4 - \omega_{m,1}x_3 \\ & - \chi x_{21} + \Lambda_1 x_{14} + \Lambda_1^* x_{13}, \end{aligned} \quad (\text{C9})$$

$$\begin{aligned} \dot{x}_{10} = & -\frac{\gamma_{m,1}}{2}x_{10} - \frac{\gamma_{m,1}}{2}x_9 + \omega_{m,1}x_4 - \omega_{m,1}x_3 \\ & - \chi x_{21} + \Lambda_1 x_{14} + \Lambda_1^* x_{13}, \end{aligned} \quad (\text{C10})$$

$$\begin{aligned} \dot{x}_{11} = & -\frac{\gamma_{m,2}}{2}x_{11} - \frac{\gamma_{m,2}}{2}x_{12} + \omega_{m,2}x_6 - \omega_{m,2}x_5 \\ & - \chi x_{21} + \Lambda_2 x_{18} + \Lambda_2^* x_{17}, \end{aligned} \quad (\text{C11})$$

$$\begin{aligned} \dot{x}_{12} = & -\frac{\gamma_{m,2}}{2}x_{12} - \frac{\gamma_{m,2}}{2}x_{11} + \omega_{m,2}x_6 - \omega_{m,2}x_5 \\ & - \chi x_{21} + \Lambda_2 x_{18} + \Lambda_2^* x_{17}, \end{aligned} \quad (\text{C12})$$

$$\dot{x}_{13} = -\left(i\Delta_s + \frac{\kappa}{2}\right)x_{13} + \omega_{m,1}x_{15} + i\Lambda_1 x_3 + i\Lambda_2 x_{21}, \quad (\text{C13})$$

$$\dot{x}_{14} = \left(i\Delta_s - \frac{\kappa}{2}\right)x_{14} + \omega_{m,1}x_{16} - i\Lambda_1^* x_3 - i\Lambda_2^* x_{21}, \quad (\text{C14})$$

$$\begin{aligned} \dot{x}_{15} = & -\left(i\Delta_s + \gamma_{m,1} + \frac{\kappa}{2}\right)x_{15} - \omega_{m,1}x_{13} + i\Lambda_1 x_{10} \\ & + i\Lambda_2 x_{24} - \chi x_{17}, \end{aligned} \quad (\text{C15})$$

$$\begin{aligned} \dot{x}_{16} = & \left(i\Delta_s - \gamma_{m,1} - \frac{\kappa}{2}\right)x_{16} - \omega_{m,1}x_{14} - i\Lambda_1^* x_{10} \\ & - i\Lambda_2^* x_{24} - \chi x_{18}, \end{aligned} \quad (\text{C16})$$

$$\dot{x}_{17} = -\left(i\Delta_s + \frac{\kappa}{2}\right)x_{17} + \omega_{m,1}x_{19} + i\Lambda_1 x_{21} + i\Lambda_2 x_5, \quad (\text{C17})$$

$$\dot{x}_{18} = \left(i\Delta_s - \frac{\kappa}{2}\right)x_{18} + \omega_{m,1}x_{20} - i\Lambda_1^* x_{21} - i\Lambda_2^* x_5, \quad (\text{C18})$$

$$\begin{aligned} \dot{x}_{19} = & - \left(i\Delta_s + \gamma_{m,2} + \frac{\kappa}{2} \right) x_{19} - \omega_{m,2}x_{17} + i\Lambda_1x_{23} \\ & + i\Lambda_2x_{12} - \chi x_{13}, \end{aligned} \quad (\text{C19})$$

$$\begin{aligned} \dot{x}_{20} = & \left(i\Delta_s - \gamma_{m,2} - \frac{\kappa}{2} \right) x_{20} - \omega_{m,2}x_{18} - i\Lambda_1^*x_{23} \\ & - i\Lambda_2^*x_{12} - \chi x_{14}, \end{aligned} \quad (\text{C20})$$

$$\dot{x}_{21} = \omega_{m,1}x_{24} + \omega_{m,2}x_{23}, \quad (\text{C21})$$

$$\begin{aligned} \dot{x}_{22} = & - (\gamma_{m,1} + \gamma_{m,2})x_{22} - \omega_{m,1}x_{23} - \omega_{m,2}x_{24} - \chi x_{10} \\ & - \chi x_{11} + \Lambda_1x_{20} + \Lambda_1^*x_{19} + \Lambda_2x_{16} + \Lambda_2^*x_{15}, \end{aligned} \quad (\text{C22})$$

$$\begin{aligned} \dot{x}_{23} = & - \gamma_{m,2}x_{23} + \omega_{m,1}x_{22} - \omega_{m,2}x_{21} - \chi x_3 \\ & + \Lambda_2x_{14} + \Lambda_2^*x_{13}, \end{aligned} \quad (\text{C23})$$

$$\begin{aligned} \dot{x}_{24} = & - \gamma_{m,1}x_{24} - \omega_{m,1}x_{21} + \omega_{m,2}x_{22} - \chi x_5 \\ & + \Lambda_1x_{18} + \Lambda_1^*x_{17}. \end{aligned} \quad (\text{C24})$$

By rewriting the above equations in a compact form, i.e.,

$$\dot{X} = M \cdot X + N, \quad (\text{C25})$$

and introducing the following expressions

$$\begin{aligned} \Omega_{1,\pm} &= i\Delta_s \pm \frac{\kappa}{2}, \\ \Omega_{2,\pm} &= i\Delta_s \pm \gamma_{m,1} \pm \frac{\kappa}{2}, \\ \Omega_{3,\pm} &= i\Delta_s \pm \gamma_{m,2} \pm \frac{\kappa}{2}, \end{aligned} \quad (\text{C26})$$

we have

$$\begin{aligned} N = & [0, \kappa, 0, 2\gamma_{m,1}\bar{n}_{m,1}, 0, 2\gamma_{m,2}\bar{n}_{m,2}, 0, 0, \\ & 0, 0, 0, 0, 0, 0, 0, 0, 0, 0, 0, 0, 0, 0]^T, \end{aligned} \quad (\text{C27})$$

and

$M =$

$$\begin{pmatrix}
 -\kappa & 0 & 0 & 0 & 0 & 0 & 0 & 0 & 0 & 0 & 0 & 0 & 0 & -i\Lambda_1^* & i\Lambda_1 & 0 & 0 \\
 -i\Lambda_2^* & i\Lambda_2 & 0 & 0 & 0 & 0 & 0 & 0 & 0 & 0 & 0 & 0 & 0 & -i\Lambda_1^* & i\Lambda_1 & 0 & 0 \\
 0 & -\kappa & 0 & 0 & 0 & 0 & 0 & 0 & 0 & 0 & 0 & 0 & 0 & -i\Lambda_1^* & i\Lambda_1 & 0 & 0 \\
 -i\Lambda_2^* & i\Lambda_2 & 0 & 0 & 0 & 0 & 0 & 0 & 0 & 0 & 0 & 0 & 0 & -i\Lambda_1^* & i\Lambda_1 & 0 & 0 \\
 0 & 0 & 0 & 0 & 0 & 0 & 0 & 0 & 2\omega_{m,1} & 2\omega_{m,1} & 0 & 0 & 0 & 0 & 0 & 0 & 0 \\
 0 & 0 & 0 & 0 & 0 & 0 & 0 & 0 & 0 & 0 & 0 & 0 & 0 & 0 & 0 & 0 & 0 \\
 0 & 0 & 0 & -2\gamma_{m,1} & 0 & 0 & 0 & 0 & -2\omega_{m,1} & -2\omega_{m,1} & 0 & 0 & 0 & 0 & 2\Lambda_1^* & 2\Lambda_1 & 0 \\
 0 & 0 & 0 & 0 & 0 & 0 & 0 & -2\chi & 0 & 0 & 0 & 0 & 0 & 0 & 0 & 0 & 0 \\
 0 & 0 & 0 & 0 & 0 & 0 & 0 & 0 & 0 & 0 & 2\omega_{m,2} & 2\omega_{m,2} & 0 & 0 & 0 & 0 & 0 \\
 0 & 0 & 0 & 0 & 0 & 0 & 0 & 0 & 0 & 0 & 0 & 0 & 0 & 0 & 0 & 0 & 0 \\
 0 & 0 & 0 & 0 & 0 & -2\gamma_{m,2} & 0 & 0 & 0 & 0 & -2\omega_{m,2} & -2\omega_{m,2} & 0 & 0 & 0 & 0 & 0 \\
 0 & 0 & 2\Lambda_2^* & 2\Lambda_2 & 0 & 0 & -2\chi & 0 & 0 & 0 & 0 & 0 & 0 & 0 & 0 & 0 & 0 \\
 0 & 0 & 0 & 0 & 0 & 0 & 0 & -2\Omega_{1,+} & 0 & 0 & 0 & 0 & 0 & 2i\Lambda_1 & 0 & 0 & 0 \\
 2i\Lambda_2 & 0 & 0 & 0 & 0 & 0 & 0 & 0 & 0 & 0 & 0 & 0 & 0 & 0 & 0 & 0 & 0 \\
 0 & 0 & 0 & 0 & 0 & 0 & 0 & 2\Omega_{1,-} & 0 & 0 & 0 & 0 & 0 & 0 & -2i\Lambda_1^* & 0 & 0 \\
 0 & -2i\Lambda_2^* & 0 & 0 & 0 & 0 & 0 & 0 & 0 & 0 & 0 & 0 & 0 & 0 & 0 & 0 & 0 \\
 0 & 0 & -\omega_{m,1} & \omega_{m,1} & 0 & 0 & 0 & 0 & -\gamma_{m,1}/2 & -\gamma_{m,1}/2 & 0 & 0 & \Lambda_1^* & \Lambda_1 & 0 & 0 & 0 \\
 0 & 0 & 0 & 0 & -\chi & 0 & 0 & 0 & 0 & 0 & 0 & 0 & \Lambda_1^* & \Lambda_1 & 0 & 0 & 0 \\
 0 & 0 & -\omega_{m,1} & \omega_{m,1} & 0 & 0 & 0 & 0 & -\gamma_{m,1}/2 & -\gamma_{m,1}/2 & 0 & 0 & \Lambda_1^* & \Lambda_1 & 0 & 0 & 0 \\
 0 & 0 & 0 & 0 & -\chi & 0 & 0 & 0 & 0 & 0 & 0 & 0 & \Lambda_1^* & \Lambda_1 & 0 & 0 & 0 \\
 \Lambda_2^* & \Lambda_2 & 0 & 0 & -\omega_{m,2} & \omega_{m,2} & 0 & 0 & 0 & 0 & -\gamma_{m,2}/2 & -\gamma_{m,2}/2 & 0 & 0 & 0 & 0 & 0 \\
 0 & 0 & 0 & 0 & -\chi & 0 & 0 & 0 & 0 & 0 & 0 & 0 & 0 & 0 & 0 & 0 & 0 \\
 0 & 0 & 0 & 0 & -\omega_{m,2} & \omega_{m,2} & 0 & 0 & 0 & 0 & -\gamma_{m,2}/2 & -\gamma_{m,2}/2 & 0 & 0 & 0 & 0 & 0 \\
 \Lambda_2^* & \Lambda_2 & 0 & 0 & -\chi & 0 & 0 & 0 & 0 & 0 & 0 & 0 & 0 & 0 & 0 & 0 & 0 \\
 0 & 0 & i\Lambda_1 & 0 & 0 & 0 & 0 & 0 & 0 & 0 & 0 & 0 & -\Omega_{1,+} & 0 & \omega_{m,1} & 0 & 0 \\
 0 & 0 & 0 & 0 & i\Lambda_2 & 0 & 0 & 0 & 0 & 0 & 0 & 0 & 0 & 0 & 0 & 0 & 0 \\
 0 & 0 & -i\Lambda_1^* & 0 & 0 & 0 & 0 & 0 & 0 & 0 & 0 & 0 & 0 & \Omega_{1,-} & 0 & \omega_{m,1} & 0 \\
 0 & 0 & 0 & 0 & -i\Lambda_2^* & 0 & 0 & 0 & 0 & 0 & 0 & 0 & 0 & 0 & 0 & 0 & 0 \\
 0 & 0 & 0 & 0 & 0 & 0 & 0 & 0 & 0 & 0 & 0 & 0 & 0 & 0 & 0 & 0 & 0 \\
 -\chi & 0 & 0 & 0 & 0 & 0 & 0 & 0 & i\Lambda_2 & 0 & i\Lambda_1 & 0 & 0 & -\omega_{m,1} & 0 & -\Omega_{2,+} & 0 \\
 0 & 0 & 0 & 0 & 0 & 0 & 0 & 0 & 0 & 0 & -i\Lambda_1^* & 0 & 0 & 0 & -\omega_{m,1} & 0 & \Omega_{2,-} \\
 0 & -\chi & 0 & 0 & 0 & 0 & 0 & 0 & -i\Lambda_2^* & 0 & 0 & 0 & 0 & 0 & 0 & 0 & 0 \\
 0 & 0 & 0 & 0 & i\Lambda_2 & 0 & 0 & 0 & 0 & 0 & 0 & 0 & 0 & 0 & 0 & 0 & 0 \\
 -\Omega_{1,+} & 0 & \omega_{m,1} & 0 & i\Lambda_1 & 0 & 0 & 0 & 0 & 0 & 0 & 0 & 0 & 0 & 0 & 0 & 0 \\
 0 & 0 & 0 & 0 & -i\Lambda_2^* & 0 & 0 & 0 & 0 & 0 & 0 & 0 & 0 & 0 & 0 & 0 & 0 \\
 0 & \Omega_{1,-} & 0 & \omega_{m,1} & -i\Lambda_1^* & 0 & 0 & 0 & 0 & 0 & 0 & 0 & 0 & 0 & 0 & 0 & 0 \\
 0 & 0 & 0 & 0 & 0 & 0 & 0 & 0 & 0 & 0 & 0 & 0 & i\Lambda_2 & -\chi & 0 & 0 & 0 \\
 -\omega_{m,2} & 0 & -\Omega_{3,+} & 0 & 0 & 0 & 0 & 0 & i\Lambda_1 & 0 & 0 & 0 & 0 & 0 & 0 & 0 & 0 \\
 0 & 0 & 0 & 0 & 0 & 0 & 0 & 0 & 0 & 0 & 0 & 0 & -i\Lambda_2^* & 0 & -\chi & 0 & 0 \\
 0 & -\omega_{m,2} & 0 & \Omega_{3,-} & 0 & 0 & 0 & 0 & -i\Lambda_1^* & 0 & 0 & 0 & 0 & 0 & 0 & 0 & 0 \\
 0 & 0 & 0 & 0 & 0 & 0 & 0 & 0 & 0 & 0 & 0 & 0 & 0 & 0 & 0 & 0 & 0 \\
 0 & 0 & 0 & 0 & 0 & 0 & 0 & \omega_{m,2} & \omega_{m,1} & 0 & 0 & 0 & 0 & 0 & 0 & 0 & 0 \\
 0 & 0 & 0 & 0 & 0 & 0 & 0 & 0 & 0 & 0 & -\chi & -\chi & 0 & 0 & 0 & \Lambda_2^* & \Lambda_2 \\
 0 & 0 & \Lambda_1^* & \Lambda_1 & 0 & -\gamma_{m,1}-\gamma_{m,2} & -\omega_{m,1} & -\omega_{m,2} & 0 & 0 & 0 & 0 & 0 & 0 & 0 & 0 & 0 \\
 0 & 0 & -\chi & 0 & 0 & 0 & 0 & 0 & 0 & 0 & 0 & 0 & 0 & 0 & \Lambda_2^* & \Lambda_2 & 0 \\
 0 & 0 & 0 & 0 & -\omega_{m,2} & \omega_{m,1} & -\gamma_{m,2} & 0 & 0 & 0 & 0 & 0 & 0 & 0 & 0 & 0 & 0 \\
 0 & 0 & 0 & 0 & -\chi & 0 & 0 & 0 & 0 & 0 & 0 & 0 & 0 & 0 & 0 & 0 & 0 \\
 \Lambda_1^* & \Lambda_1 & 0 & 0 & -\omega_{m,1} & \omega_{m,2} & 0 & -\gamma_{m,1} & 0 & 0 & 0 & 0 & 0 & 0 & 0 & 0 & 0
 \end{pmatrix}$$

- [1] R. Horodecki, P. Horodecki, M. Horodecki, and K. Horodecki, "Quantum entanglement," *Rev. Mod. Phys.* **81**, 865 (2009).
- [2] E. Schrödinger, "Discussion of Probability Relations between Separated Systems," *Math. Proc. Camb. Phil. Soc.* **31**, 555 (1935).
- [3] A. Einstein, B. Podolsky, and N. Rosen, "Can Quantum-Mechanical Description of Physical Reality Be Considered Complete?" *Phys. Rev.* **47**, 777 (1935).
- [4] M. D. Reid, "Demonstration of the Einstein-Podolsky-Rosen

paradox using nondegenerate parametric amplification," *Phys. Rev. A* **40**, 913 (1989).

- [5] Z. Y. Ou, S. F. Pereira, H. J. Kimble, and K. C. Peng, "Realization of the Einstein-Podolsky-Rosen paradox for continuous variables," *Phys. Rev. Lett.* **68**, 3663 (1992).
- [6] H. M. Wiseman, S. J. Jones, and A. C. Doherty, "Steering, Entanglement, Nonlocality, and the Einstein-Podolsky-Rosen Paradox," *Phys. Rev. Lett.* **98**, 140402 (2007).
- [7] Q. Y. He, Q. H. Gong, and M. D. Reid, "Classifying Direc-

- tional Gaussian Entanglement, Einstein-Podolsky-Rosen Steering, and Discord,” *Phys. Rev. Lett.* **114**, 060402 (2015).
- [8] Yu Xiang, Shuming Cheng, Qihuang Gong, Zbigniew Ficek, and Qiongyi He, “Quantum Steering: Practical Challenges and Future Directions,” *PRX Quantum* **3**, 030102 (2022).
- [9] C. Branciard, E. G. Cavalanti, S. P. Walborn, V. Scarani, and H. M. Wiseman, “One-sided device-independent quantum key distribution: Security, feasibility, and the connection with steering,” *Phys. Rev. A* **85**, 010301 (2012).
- [10] N. Walk, S. Hosseini, J. Geng, O. Thearle, J. Y. Haw, S. Armstrong, S. M. Assad, J. Janousek, T. C. Ralph, T. Symul, H. M. Wiseman, and P. K. Lam, “Experimental demonstration of Gaussian protocols for one-sided device-independent quantum key distribution,” *Optica* **3**, 634 (2016).
- [11] Y. Li, Y. Xiang, X.-D. Yu, H. C. Nguyen, O. Gühne, and Q.-Y. He, “Randomness Certification from Multipartite Quantum Steering for Arbitrary Dimensional Systems,” *Phys. Rev. Lett.* **132**, 080201 (2024).
- [12] Q.-Y. He, L. Rosales-Zárate, G. Adesso, and M. D. Reid, “Secure Continuous Variable Teleportation and Einstein-Podolsky-Rosen Steering,” *Phys. Rev. Lett.* **115**, 180502 (2015).
- [13] C.-Y. Chiu, N. Lambert, T.-L. Liao, F. Nori, and C.-M. Li, “No-cloning of quantum steering,” *npj Quantum Inf.* **2**, 16020 (2016).
- [14] R. Simon, “Peres-Horodecki Separability Criterion for Continuous Variable Systems,” *Phys. Rev. Lett.* **84**, 2726 (2000).
- [15] G. Adesso, A. Serafini, and F. Illuminati, “Extremal entanglement and mixedness in continuous variable systems,” *Phys. Rev. A* **70**, 022318 (2004).
- [16] G. Adesso and F. Illuminati, “Entanglement in continuous-variable systems: recent advances and current perspectives,” *J. Phys. A* **40**, 7821 (2007).
- [17] I. Kogias, A. R. Lee, S. Ragy, and G. Adesso, “Quantification of Gaussian Quantum Steering,” *Phys. Rev. Lett.* **114**, 060403 (2015).
- [18] X.-L. Wang, L.-K. Chen, W. Li, H.-L. Huang, C. Liu, C. Chen, Y.-H. Luo, Z.-E. Su, D. Wu, Z.-D. Li, H. Lu, Y. Hu, X. Jiang, C.-Z. Peng, L. Li, N.-L. Liu, Y.-A. Chen, C.-Y. Lu, and J.-W. Pan, “Experimental Ten-Photon Entanglement,” *Phys. Rev. Lett.* **117**, 210502 (2016).
- [19] A. Stute, B. Casabone, P. Schindler, T. Monz, P. O. Schmidt, B. Brandstatter, T. E. Northup, and R. Blatt, “Tunable ion-photon entanglement in an optical cavity,” *Nature (London)* **485**, 482 (2012).
- [20] T. van Leent, M. Bock, F. Fertig, R. Garthoff, S. Eppelt, Y. Zhou, P. Malik, M. Seubert, T. Bauer, W. Rosenfeld, C. Becher, and H. Weinfurter, “Entangling single atoms over 33 km telecom fibre,” *Nature (London)* **607**, 69 (2022).
- [21] P. Kurpiers, P. Magnard, T. Walter, B. Royer, M. Pechal, J. Heinsoo, Y. Salathé, A. Akin, S. Storz, J.-C. Besse, S. Gasparinetti, A. Blais, and A. Wallraff, “Deterministic quantum state transfer and remote entanglement using microwave photons,” *Nature (London)* **558**, 264 (2018).
- [22] T. A. Palomaki, J. D. Teufel, R. W. Simmonds, and K. W. Lehnert, “Entangling Mechanical Motion with Microwave Fields,” *Science* **342**, 710 (2013).
- [23] S. Kotler, G. A. Peterson, E. Shojaei, F. Lecocq, K. Cicak, A. Kwiatkowski, S. Geller, S. Glancy, E. Knill, R. W. Simmonds, J. Aumentado, and J. D. Teufel, “Direct observation of deterministic macroscopic entanglement,” *Science* **372**, 622 (2021).
- [24] L. Mercier de Lépinay, C. F. Ockeloen-Korppi, M.-J. Woolley, and M. A. Sillanpää, “Quantum mechanics-free subsystem with mechanical oscillators,” *Science* **372**, 625 (2021).
- [25] D.-G. Lai, J.-Q. Liao, A. Miranowicz, and F. Nori, “Noise-Tolerant Optomechanical Entanglement via Synthetic Magnetism,” *Phys. Rev. Lett.* **129**, 063602 (2022).
- [26] J.-X. Liu, Y.-F. Jiao, Y. Li, X.-W. Xu, Q.-Y. He, and H. Jing, “Phase-controlled asymmetric optomechanical entanglement against optical backscattering,” *Sci. China Phys. Mech. Astron.* **66**, 230312 (2023).
- [27] Y.-D. Wang and A. A. Clerk, “Reservoir-Engineered Entanglement in Optomechanical Systems,” *Phys. Rev. Lett.* **110**, 253601 (2013).
- [28] C.-J. Yang, J.-H. An, W. Yang, and Y. Li, “Generation of stable entanglement between two cavity mirrors by squeezed-reservoir engineering,” *Phys. Rev. A* **92**, 062311 (2015).
- [29] Y.-F. Jiao, Y.-L. Zuo, Y. Wang, W. Lu, J.-Q. Liao, L.-M. Kuang, and H. Jing, “Tripartite Quantum Entanglement with Squeezed Optomechanics,” *Laser Photonics Rev.* **2301154**.
- [30] D.-G. Lai, Y.-H. Chen, W. Qin, A. Miranowicz, and F. Nori, “Tripartite optomechanical entanglement via optical-dark-mode control,” *Phys. Rev. Res.* **4**, 033112 (2022).
- [31] J. Huang, D.-G. Lai, and J.-Q. Liao, “Thermal-noise-resistant optomechanical entanglement via general dark-mode control,” *Phys. Rev. A* **106**, 063506 (2022).
- [32] J. Li, G. Li, S. Zippilli, D. Vitali, and T. Zhang, “Enhanced entanglement of two different mechanical resonators via coherent feedback,” *Phys. Rev. A* **95**, 043819 (2017).
- [33] M. Ho, E. Oudot, J.-D. Bancal, and N. Sangouard, “Witnessing Optomechanical Entanglement with Photon Counting,” *Phys. Rev. Lett.* **121**, 023602 (2018).
- [34] M. Wang, X.-Y. Lü, Y.-D. Wang, J.-Q. You, and Y. Wu, “Macroscopic quantum entanglement in modulated optomechanics,” *Phys. Rev. A* **94**, 053807 (2016).
- [35] J. Yang, T.-X. Lu, M. Peng, J. Liu, Y.-F. Jiao, and H. Jing, “Multi-field-driven optomechanical entanglement,” *Opt. Express* **32**, 785 (2024).
- [36] Y.-F. Jiao, S.-D. Zhang, Y.-L. Zhang, A. Miranowicz, L.-M. Kuang, and H. Jing, “Nonreciprocal Optomechanical Entanglement against Backscattering Losses,” *Phys. Rev. Lett.* **125**, 143605 (2020).
- [37] Y.-F. Jiao, J.-X. Liu, Y. Li, R. Yang, L.-M. Kuang, and H. Jing, “Nonreciprocal Enhancement of Remote Entanglement between Nonidentical Mechanical Oscillators,” *Phys. Rev. Applied* **18**, 064008 (2022).
- [38] Z.-H. Huang, Y.-F. Jiao, L.-L. Yan, D.-Y. Wang, S.-L. Su, and H. Jing, “Nonreciprocal enhancement of macroscopic entanglement with noise tolerance,” *Phys. Rev. A* **110**, 012423 (2024).
- [39] D. L. Sounas and A. Alù, “Non-reciprocal photonics based on time modulation,” *Nat. Photonics* **11**, 774 (2017).
- [40] Y. Shoji and T. Mizumoto, “Magneto-optical non-reciprocal devices in silicon photonics,” *Sci. Technol. Adv. Mater.* **15**, 014602 (2014).
- [41] C. Caloz, A. Alù, S. Tretyakov, D. Sounas, K. Achouri, and Z.-L. Deck-Léger, “Electromagnetic Nonreciprocity,” *Phys. Rev. Applied* **10**, 047001 (2018).
- [42] S. Zhang, Y. Hu, G. Lin, Y. Niu, K. Xia, J. Gong, and S. Gong, “Thermal-motion-induced non-reciprocal quantum optical system,” *Nat. Photonics* **12**, 744 (2018).
- [43] P. Yang, X. Xia, H. He, S. Li, X. Han, P. Zhang, G. Li, P. Zhang, J. Xu, Y. Yang, and T. Zhang, “Realization of Nonlinear Optical Nonreciprocity on a Few-Photon Level Based on Atoms Strongly Coupled to an Asymmetric Cavity,” *Phys. Rev. Lett.* **123**, 233604 (2019).
- [44] C. Liang, B. Liu, A.-N. Xu, X. Wen, C. Lu, K. Xia, M. K. Tey, Y.-C. Liu, and L. You, “Collision-Induced Broadband Optical Nonreciprocity,” *Phys. Rev. Lett.* **125**, 123901 (2020).

- [45] C.-H. Dong, Z. Shen, C.-L. Zou, Y.-L. Zhang, W. Fu, and G.-C. Guo, “Brillouin-scattering-induced transparency and nonreciprocal light storage,” *Nat. Commun.* **6**, 6193 (2015).
- [46] K. Xia, F. Nori, and M. Xiao, “Cavity-Free Optical Isolators and Circulators Using a Chiral Cross-Kerr Nonlinearity,” *Phys. Rev. Lett.* **121**, 203602 (2018).
- [47] A. Rosario Hamann, C. Müller, M. Jerger, M. Zanner, J. Combes, M. Pletyukhov, M. Weides, T. M. Stace, and A. Fedorov, “Nonreciprocity Realized with Quantum Nonlinearity,” *Phys. Rev. Lett.* **121**, 123601 (2018).
- [48] S. Manipatruni, J. T. Robinson, and M. Lipson, “Optical Nonreciprocity in Optomechanical Structures,” *Phys. Rev. Lett.* **102**, 213903 (2009).
- [49] Z. Shen, Y.-L. Zhang, Y. Chen, C.-L. Zou, Y.-F. Xiao, X.-B. Zou, F.-W. Sun, G.-C. Guo, and C.-H. Dong, “Experimental realization of optomechanically induced non-reciprocity,” *Nat. Photonics* **10**, 657 (2016).
- [50] N. R. Bernier, L. D. Tóth, A. Koottandavida, M. A. Ioannou, D. Malz, A. Nunnenkamp, A. K. Feofanov, and T. J. Kippenberg, “Nonreciprocal reconfigurable microwave optomechanical circuit,” *Nat. Commun.* **8**, 604 (2017).
- [51] B. Peng, Ş. K. Özdemir, F. Lei, F. Monifi, M. Gianfreda, G.-L. Long, S. Fan, F. Nori, C. M. Bender, and L. Yang, “Parity-time-symmetric whispering-gallery microcavities,” *Nat. Phys.* **10**, 394 (2014).
- [52] L. Chang, X. Jiang, S. Hua, C. Yang, J. Wen, L. Jiang, G. Li, G. Wang, and M. Xiao, “Parity-time symmetry and variable optical isolation in active-passive-coupled microresonators,” *Nat. Photonics* **8**, 524 (2014).
- [53] D.-W. Wang, H.-T. Zhou, M.-J. Guo, J.-X. Zhang, J. Evers, and S.-Y. Zhu, “Optical Diode Made from a Moving Photonic Crystal,” *Phys. Rev. Lett.* **110**, 093901 (2013).
- [54] H. Lü, Y. Jiang, Y.-Z. Wang, and H. Jing, “Optomechanically induced transparency in a spinning resonator,” *Photon. Res.* **5**, 367 (2017).
- [55] S. Maayani, R. Dahan, Y. Kligerman, E. Moses, A. U. Hassan, H. Jing, F. Nori, D. N. Christodoulides, and T. Carmon, “Flying couplers above spinning resonators generate irreversible refraction,” *Nature (London)* **558**, 569 (2018).
- [56] L. Tang, J. Tang, M. Chen, F. Nori, M. Xiao, and K. Xia, “Quantum Squeezing Induced Optical Nonreciprocity,” *Phys. Rev. Lett.* **128**, 083604 (2022).
- [57] D.-W. Zhang, L.-L. Zheng, C. You, C.-S. Hu, Y. Wu, and X.-Y. Lü, “Nonreciprocal chaos in a spinning optomechanical resonator,” *Phys. Rev. A* **104**, 033522 (2021).
- [58] B. Li, Ş. K. Özdemir, X.-W. Xu, L. Zhang, L.-M. Kuang, and H. Jing, “Nonreciprocal optical solitons in a spinning Kerr resonator,” *Phys. Rev. A* **103**, 053522 (2021).
- [59] Y. Jiang, S. Maayani, T. Carmon, F. Nori, and H. Jing, “Nonreciprocal Phonon Laser,” *Phys. Rev. Applied* **10**, 064037 (2018).
- [60] K.-W. Huang, Y. Wu, and L.-G. Si, “Parametric-amplification-induced nonreciprocal magnon laser,” *Opt. Lett.* **47**, 3311 (2022).
- [61] W.-A. Li, G.-Y. Huang, J.-P. Chen, and Y. Chen, “Nonreciprocal enhancement of optomechanical second-order sidebands in a spinning resonator,” *Phys. Rev. A* **102**, 033526 (2020).
- [62] R. Huang, A. Miranowicz, J.-Q. Liao, F. Nori, and H. Jing, “Nonreciprocal Photon Blockade,” *Phys. Rev. Lett.* **121**, 153601 (2018).
- [63] P. Yang, M. Li, X. Han, H. He, G. Li, C.-L. Zou, P. Zhang, Y. Qian, and T. Zhang, “Non-Reciprocal Cavity Polariton with Atoms Strongly Coupled to Optical Cavity,” *Laser Photonics Rev.* **17**, 2200574 (2023).
- [64] D.-Y. Wang, L.-L. Yan, S.-L. Su, C.-H. Bai, H.-F. Wang, and E. Liang, “Squeezing-induced nonreciprocal photon blockade in an optomechanical microresonator,” *Opt. Express* **31**, 22343 (2023).
- [65] Y. Wang, W. Xiong, Z. Xu, G.-Q. Zhang, and J.-Q. You, “Dissipation-induced nonreciprocal magnon blockade in a magnon-based hybrid system,” *Sci. China Phys. Mech. Astron.* **65**, 260314 (2022).
- [66] L. Orr, S. A. Khan, N. Buchholz, S. Kotler, and A. Metelmann, “High-Purity Entanglement of Hot Propagating Modes Using Nonreciprocity,” *PRX Quantum* **4**, 020344 (2023).
- [67] C.-P. Shen, J.-Q. Chen, X.-F. Pan, Y.-M. Ren, X.-L. Dong, X.-L. Hei, Y.-F. Qiao, and P.-B. Li, “Tunable nonreciprocal photon correlations induced by directional quantum squeezing,” *Phys. Rev. A* **108**, 023716 (2023).
- [68] Q. Bin, H. Jing, Y. Wu, F. Nori, and X.-Y. Lü, “Nonreciprocal Bundle Emissions of Quantum Entangled Pairs,” *Phys. Rev. Lett.* **133**, 043601 (2024).
- [69] M. Fruchart, R. Hanai, P. B. Littlewood, and V. Vitelli, “Nonreciprocal phase transitions,” *Nature* **592**, 363 (2021).
- [70] G.-L. Zhu, C.-S. Hu, H. Wang, W. Qin, X.-Y. Lü, and F. Nori, “Nonreciprocal Superradiant Phase Transitions and Multicriticality in a Cavity QED System,” *Phys. Rev. Lett.* **132**, 193602 (2024).
- [71] S.-Y. Guan, H.-F. Wang, and X.-X. Yi, “Manipulation of tunable nonreciprocal entanglement and one-way steering induced by two-photon driving,” *Phys. Rev. A* **109**, 062423 (2024).
- [72] S.-X. Wu, C.-H. Bai, G. Li, C.-S. Yu, and T. Zhang, “Quantum squeezing-induced quantum entanglement and EPR steering in a coupled optomechanical system,” *Opt. Express* **32**, 260 (2024).
- [73] W. Zhong, Q. Zheng, G. Cheng, and A. Chen, “Nonreciprocal genuine steering of three macroscopic samples in a spinning microwave magnon system,” *Appl. Phys. Lett.* **123**, 134003 (2023).
- [74] S. Xie, R. Pennetta, and P. St. J. Russell, “Self-alignment of glass fiber nanospike by optomechanical back-action in hollow-core photonic crystal fiber,” *Optica* **3**, 277 (2016).
- [75] S. Xie, R. Pennetta, Z. Wang, and P. St. J. Russell, “Sustained Self-Starting Orbital Motion of a Glass-Fiber Nanospine Driven by Photophoretic Forces,” *ACS Photonics* **6**, 3315 (2019).
- [76] R. Pennetta, S. Xie, R. Zeltner, J. Hammer, and P. St. J. Russell, “Optomechanical cooling and self-stabilization of a waveguide coupled to a whispering-gallery-mode resonator,” *Photon. Res.* **8**, 844 (2020).
- [77] A. B. Shkarin, N. E. Flowers-Jacobs, S. W. Hoch, A. D. Kashkanova, C. Deutsch, J. Reichel, and J. G. E. Harris, “Optically Mediated Hybridization between Two Mechanical Modes,” *Phys. Rev. Lett.* **112**, 013602 (2014).
- [78] Q. Lin, J. Rosenberg, D. Chang, R. Camacho, M. Eichenfield, K. J. Vahala, and O. Painter, “Coherent mixing of mechanical excitations in nano-optomechanical structures,” *Nat. Photonics* **4**, 236 (2010).
- [79] X.-Y. Lü, Y. Wu, J. R. Johansson, H. Jing, J. Zhang, and F. Nori, “Squeezed Optomechanics with Phase-Matched Amplification and Dissipation,” *Phys. Rev. Lett.* **114**, 093602 (2015).
- [80] T. Kashiwazaki, N. Takashi, T. Yamashita, T. Kazama, K. Enbutsu, R. Kasahara, T. Umeki, and A. Furusawa, “Continuous-wave 6-dB-squeezed light with 2.5-THz-bandwidth from single-mode PPLN waveguide,” *APL Photonics* **5**, 036104 (2020).
- [81] C. W. Gardiner and P. Zoller, *Quantum Noise* (Springer, Berlin, 2000).

